TABLE 1. Viral Peptides Used to Generate Virus-specific CD8+ T Cells

Virus	Protein	Epitope	Sequence	Restriction	Donors
CMV	pp65	341-349	QYDPVAALF	HLA-A*24:02	1, 2, 3, 4, 5
CMV	pp65	495-503	NLVPMVATV	HLA-A*02:01	1, 2, 6
CMV	pp65	417-426	TPRVTGGGAM	HLA-B*07:02	7
CMV	pp65	123-131	IPSINVHHY	HLA-B*35:01	1
EBV	EBNA3A	246-254	RYSIFFDYM	HLA-A*24:02	1, 2, 5, 8, 9
AdV	Hexon	37-45	TYFSLNNKF	HLA-A*24:02	1, 3, 4

AdV indicates adenovirus; CMV, cytomegalovirus; EBV, Epstein-Barr virus.

anti-4-1BB antibodies.[14] Although extensive clinical studies have been conducted using these antibodies,[14,15] their efficacy in generating VSTs for adoptive therapy has not been investigated. The potential benefits of using immunostimulatory antibodies are: (1) substitution of antibodies for APCs, which would save the time and effort that are required to prepare APCs, (2) universal applicability irrespective of the patients' HLA types, (3) easy applicability to clinical settings due to the lack of requirements for virus vectors, (4) more uniform quality of the antibodies compared with APCs, and (5) capability of providing sufficient costimulatory signals to T cells, which might not be possible when PBMCs are stimulated with viral peptides alone. In the current study, we investigated the efficacy of anti-CD28 and anti-4-1BB antibodies for the generation of VSTs for adoptive therapy. We found that anti-4-1BB antibody significantly increases the expansion of VSTs ex vivo without causing excessive differentiation or functional deterioration of the generated T cells. The use of this anti-4-1BB antibody may pave the way for a novel strategy to generate VSTs for adoptive therapy.

MATERIALS AND METHODS

Donor Cells and Cell Lines

PBMCs from 9 healthy volunteer donors were obtained after informed consent. The donors were tested for immunity to the target virus.

EBV-transformed B-lymphoblastoid cell lines were generated by infection of PBMCs from healthy donors with concentrated EBV-containing supernatants of cultured B95-8 cells.[16] K562 cells were transduced with retroviruses that encode CD80 and CD86 and were selected to >90% purity by cell sorting for expression of these costimulatory ligands. CD80+ and CD86+ K562 were then transduced with retroviruses that encode a full-length HLA-A*24:02 or HLA-A*02:01 (Phoenix-Ampho System, Orbigen) and were sorted twice to obtain cells of >95% purity that expressed transduced HLA (named K562/A*24:02 and K562/A*02:01).[17] Cell lines were cultured in RPMI-1640 medium (Sigma, St Louis, MO) containing 10% fetal bovine serum.

Preparation of Autologous DCs

Autologous DCs were generated as previously described with some modifications.[18,19] PBMCs obtained from healthy volunteers were placed at a concentration of $5–10 \times 10^6$ cells per well in a 6-well plate with 2 mL of RPMI-1640 medium containing 10% human serum (referred to as culture medium) and were incubated for 90 minutes at 37°C in a humidified CO_2 incubator. After incubation, the nonadherent cells were removed by gentle washing, and the adherent cells were cultured in culture medium with 80 ng/mL granulocyte-macrophage colony-stimulating factor and 17 ng/mL interleukin (IL)-4 (MiltenyiBiotec, Auburn, CA). Fresh cytokines were added on days 3 and 5. On day 6, 10 ng/mL tumor necrosis factor-α, 2 ng/mL IL-1β (R&D Systems, Minneapolis, MN), 10 ng/mL IL-6 (MiltenyiBiotec, Auburn, CA), and 1000 ng/mL prostaglandin E2 (Cayman Chemical, Ann Arbor, MI) were added for maturation of the DCs. Autologous DCs were harvested on day 8 or 9 and were used for stimulation of PBMCs.

Viral Peptides

Minimal peptides corresponding to previously identified virus-specific CD8+ T-cell epitopes were synthesized by Medical & Biological Laboratories (Nagoya, Japan) (Table 1).

Preparation of Peptide-pulsed APCs

For preparation of peptide-pulsed APCs, the cells were washed once, resuspended in RPMI-1640 medium, and pulsed with the corresponding synthetic peptide at 5 μg/mL at room temperature for 2 hours. The cells were then washed and used for the generation of VSTs and for stimulation assays. Where indicated, peptide-pulsed APCs were irradiated before use.

Generation of Virus-specific CD8+ T Cells

PBMCs obtained from healthy volunteers were placed at a concentration of 1×10^6 cells per well in a 48-well plate with 1 mL of culture medium and were directly stimulated with peptides at a concentration of 1 μg/mL and with either the indicated concentration of agonistic antibody to costimulatory receptors (anti-CD28 antibody; MiltenyiBiotec, Auburn, CA) and/or anti-4-1BB antibody; R&D Systems, Minneapolis, MN) or isotype control antibody. As initial experiments showed that adding anti-4-1BB antibody 24 hours after peptide stimulation yielded maximum numbers of virus-specific CD8+ T cells (Fig. 1C), anti-4-1BB antibody was added to the culture at this time point unless otherwise specified. In some experiments, PBMCs were stimulated with 25 Gy-irradiated DCs that were loaded with peptides at a ratio of 10:1. A total of 25 IU/mL of recombinant human IL-2 (ProSpec-Tany Technogene, Rehovot, Israel) were added to the cultures on day 3 and every 3 or 4 days thereafter. VSTs were harvested on days 13 or 14, were counted and were used for phenotypic and functional analyses.

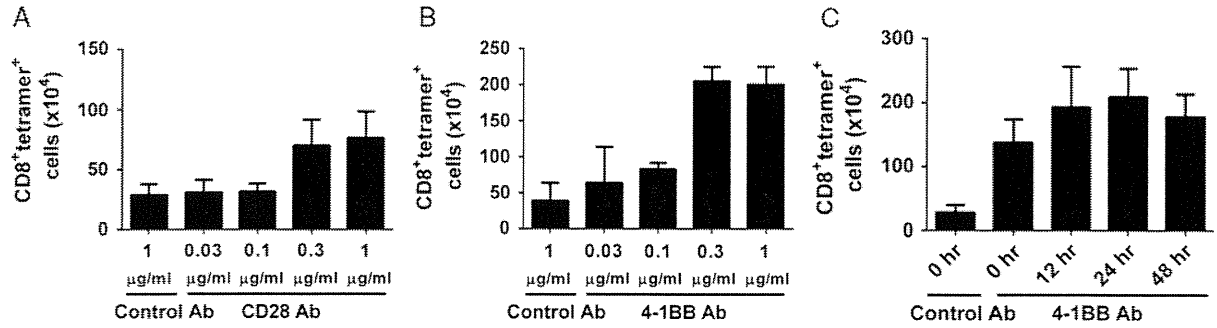

FIGURE 1. Optimization of culture conditions for the generation of virus-specific T cells using anti-CD28 or anti-4-1BB antibodies. A and B, PBMCs from healthy volunteers were stimulated with viral peptides and the indicated concentration of anti-CD28 (A) or anti-4-1BB (B) antibodies. The cells were collected on day 13, and absolute numbers of CD8+ tetramer+ cells were calculated by the formula: (the absolute number of viable cells × percentage of CD8+ tetramer+ cells among viable cells)/100. Data are representative of 8 independent experiments with 4 different virus-specific CD8+ T-cell responses. C, PBMCs were stimulated with viral peptides, and 0.3 μg/mL of anti-4-1BB antibody were added to the culture at the indicated time points after peptide stimulation. The cells were collected on day 13, and absolute numbers of CD8+ tetramer+ cells were determined. Data are representative of 6 independent experiments with 3 different virus-specific CD8+ T-cell responses. PBMCs indicates peripheral blood mononuclear cells.

Flow Cytometric Analysis

All antibodies were purchased from BD Biosciences (San Jose, CA) unless otherwise noted. The cultured T cells were analyzed for CD8, CD62L, CD45RA, CD27, CD28, and virus-specific TCRs. For the staining of virus-specific TCRs, the following phycoerythrin (PE)-conjugated HLA class I tetramers were used.

HLA-A*24:02-CMV-pp65-QYDPVAALF (QYD), HLA-A*02:01-CMV-pp65-NLVPMVATV (NLV), HLA-B*07:02-CMV-pp65-TPRVTGGGAM (TPR), HLA-B*35:01-CMV-pp65-IPSINVHHY (IPS), HLA-A*24:02-EBV-EBNA3A-RYSIFFDYM (RYS), and HLA-A*24:02-AdV-serotype 5-hexon-TYFSLNNKF (TYF) tetramers (Medical & Biological Laboratories). Data acquisition were performed with a FACSAria or FACSCanto flow cytometer (BD Biosciences), and data were analyzed using FlowJo software (TreeStar Inc., Ashland, OR).

Intracellular Cytokine Staining

Intracellular staining assays for the cytokines interferon (IFN)-γ and IL-2 were performed as previously described with some modifications.[20] In brief, cells were cocultured with peptide-pulsed or peptide-unpulsed stimulator cells and were incubated at 37°C for 6 hours. K562/A*24:02, K562/A*02:01, or autologous lymphoblastoid cell lines were used as stimulator cells for the analysis of CMV-specific and AdV-specific T cells, whereas K562/A*24:02 or K562/A*02:01 were used for the analysis of EBV-specific T cells. Brefeldin A (Golgiplug, BD Biosciences) was added during the last 4.5 hours of incubation to block the secretion of cytokines. Subsequently, the cells were fixed, permeabilized, and stained with anti-IFN-γ, anti-IL-2, and CD8 antibodies, using FIX/PERM and PERM/Wash solution (BD Biosciences). The frequency of cytokine-producing cells among CD8+ tetramer+ cells was calculated as follows: (frequency of cytokine-producing cells among CD8+ cells)/(frequency of tetramer+ cells among CD8+ cells) × 100.

CD107a Mobilization Assay

T-cell degranulation was evaluated by a CD107a mobilization assay using the IMMUNOCYTO CD107a Detection Kit (Medical & Biological Laboratories) according to the manufacturer's instructions. In brief, T cells were cocultured with peptide-pulsed or peptide-unpulsed K562/A*24:02 or K562/A*02:01 at an effector-to-target ratio of 1:1, 2 μL of anti-CD107a antibody and 2 μL of monensin in 200 μL of culture medium. After incubation for 4 hours at 37°C, the cells were stained with anti-CD8 antibody and PE-conjugated HLA class I tetramer. The frequency of CD107a+ cells among virus-specific CD8+ T cells was calculated by subtracting the background observed with the no peptide control

Carboxyfluorescein Succinimidyl Ester (CFSE) Proliferation Assay

The CFSE proliferation assay was performed as previously described with some modifications.[17] Briefly, T cells were labeled with 0.2 μM CFSE (Invitrogen, Carlsbad, CA), washed, and cocultured with peptide-pulsed or peptide-unpulsed, 25 Gy-irradiated autologous PBMCs at a ratio of 1:1 in culture medium with 5 IU/mL of recombinant human IL-2. After 120-hour incubation, the cells were stained with anti-CD8 antibody and PE-conjugated HLA class I tetramer. Division of CD8+ tetramer+ cells was assessed by CFSE dye dilution using flow cytometry.

Statistics

Differences between groups were evaluated by a 1-way analysis of variance followed by the Tukey multiple comparison tests, where appropriate. Differences were considered significant when $P < 0.05$.

RESULTS

Optimization of Culture Conditions for Generating Virus-specific CD8+ T Cells Using Anti-CD28 and Anti-4-1BB Antibodies

In the first set of experiments of VST generation, the effects of different concentrations of anti-CD28 and anti-4-1BB antibodies that were added at the time of culture initiation were examined. Addition of increasing concentrations of antibodies to PBMCs from healthy volunteers that were stimulated with viral peptides generally resulted

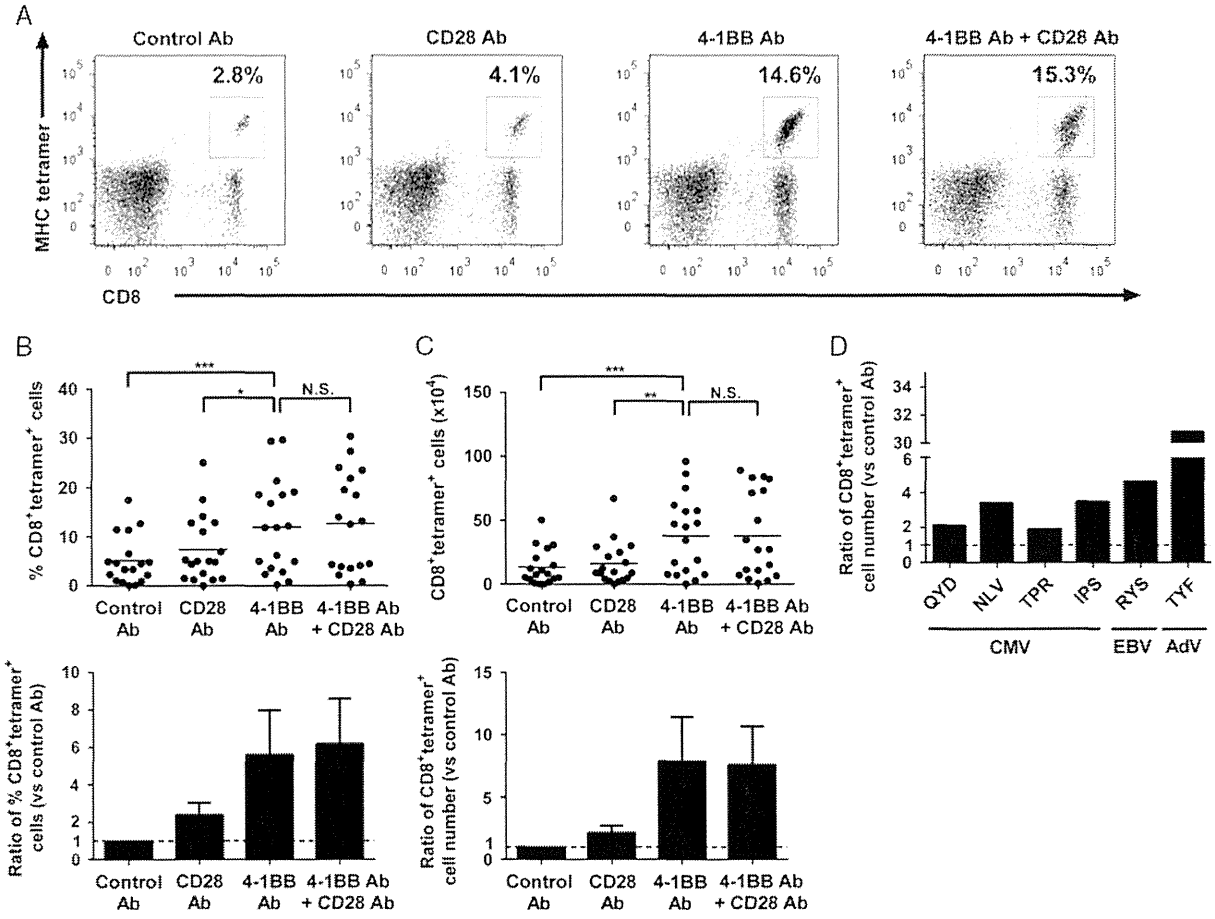

FIGURE 2. Frequencies and absolute numbers of virus-specific CD8+ T cells generated with control, anti-CD28, anti-4-1BB, or a combination of anti-CD28 and anti-4-1BB antibodies. CD8+ T cells specific for cytomegalovirus (CMV, n = 10), Epstein-Barr virus (EBV, n = 5), or adenovirus (AdV, n = 3) were generated with control, anti-CD28, anti-4-1BB, or a combination of anti-CD28 and anti-4-1BB antibodies. The concentrations of all antibodies were 0.3 μg/mL, and anti-4-1BB antibody was added 24 hours after culture initiation, as previously determined. After 13 days of culture, the cells were collected, counted, and analyzed using flow cytometry. A, Representative flow plots of the postculture cells showing the frequency of CD8+ tetramer+ cells among viable cells. Frequencies (B) and absolute numbers (C) of CD8+ tetramer+ cells. Actual values (upper panel) and the ratio of the actual values for the indicated culture conditions to those for control (lower panel) are shown for each measure. Horizontal lines in the upper panels mark the mean values. Means and SEMs are shown in the lower panels (*$P<0.05$, **$P<0.01$, ***$P<0.001$, NS, not significant, repeated measures 1-way analysis of variance followed by the Tukey multiple comparison tests). D, Ratios of absolute numbers of CD8+ tetramer+ cells generated with anti-4-1BB antibody to those generated with control antibody according to the epitopes of virus-specific T cells. Means are shown. B–D shows data pooled from more than 18 independent experiments with 18 different virus-specific CD8+ T-cell responses to CMV-pp65-QYDPVAALF (QYD), CMV-pp65-NLVPMVATV (NLV), TPRVTGGGAM (TPR), CMV-pp65-IPSINVHHY (IPS), EBV-EBNA3A-RYSIFFDYM (RYS), and AdV-serotype 5-hexon-TYFSLNNKF (TYF).

in an increased frequency and number of virus-specific CD8+ T cells, with the maximal response observed at concentrations of 0.3–1 μg/mL for both antibodies (Figs. 1A, B and data not shown). Next, as the surface expression of 4-1BB on activated T cells reaches its peak at about 24–48 hours poststimulation and has declined by 4–5 days,[21,22] we investigated the optimal time of addition of anti-4-1BB antibody to the culture. Addition of anti-4-1BB antibody 24 hours after culture initiation yielded the highest frequency and number of virus-specific CD8+ T cells (Fig. 1C and data not shown). Therefore, for subsequent experiments, anti-4-1BB antibody was added at a concentration of 0.3 μg/mL 24 hours after culture initiation, whereas anti-CD28 antibody was added at a concentration of 0.3 μg/mL at the time of culture initiation.

Effect of Anti-CD28 and Anti-4-1BB Antibodies on the Number of Virus-specific CD8+ T Cells Generated

To evaluate and compare the effects of anti-CD28 and anti-4-1BB antibodies, CD8+ T cells specific for CMV-pp65-QYD (n = 5), CMV-pp65-NLV (n = 3), CMV-pp65-TPR (n = 1), CMV-pp65-IPS (n = 1), EBV-EBNA3A-RYS (n = 5), or AdV-hexon-TYF (n = 3) epitopes were generated by stimulating PBMCs with viral peptides and with either control, anti-CD28, anti-4-1BB, or

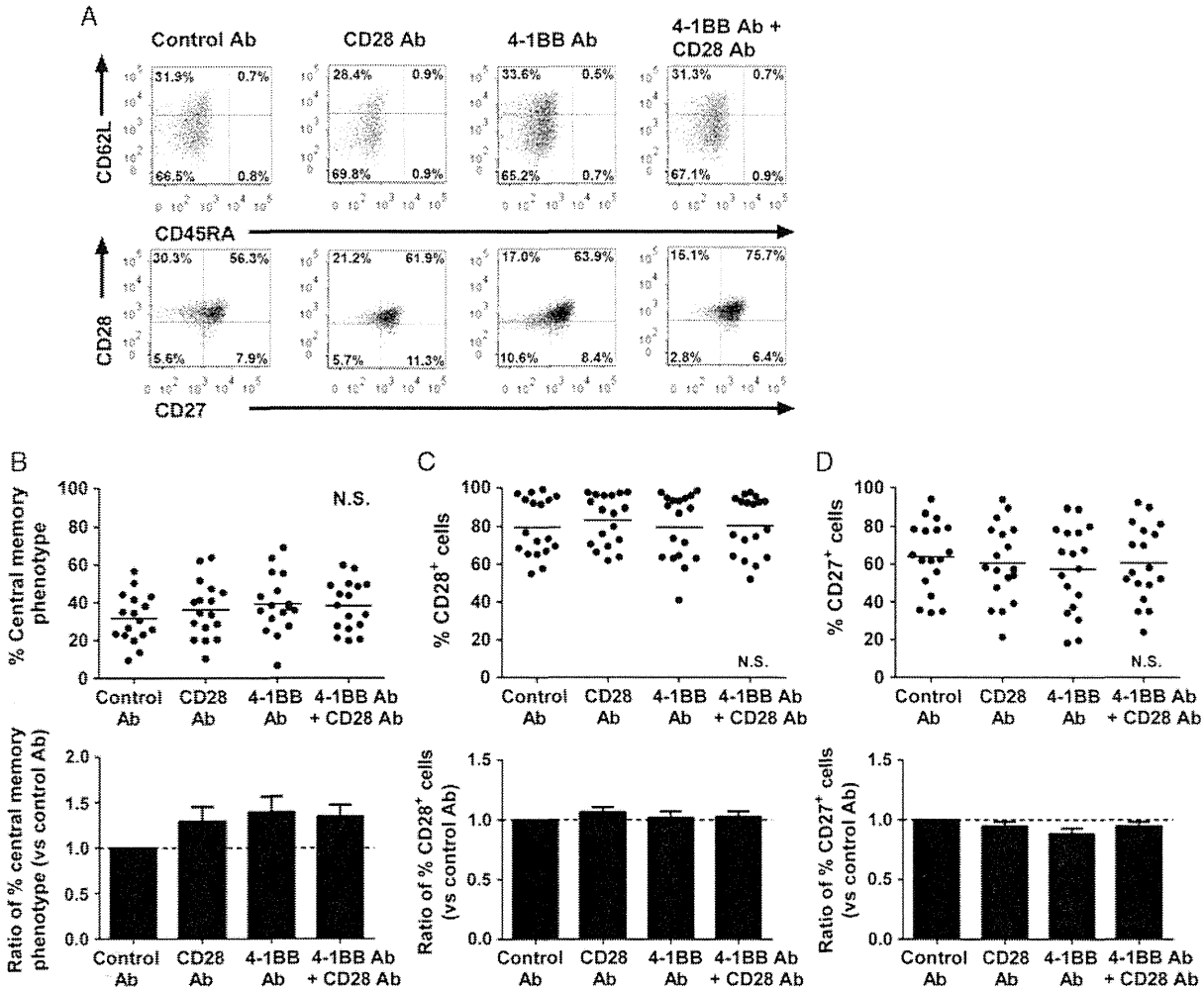

FIGURE 3. Phenotypes of virus-specific CD8+ T cells generated with control, anti-CD28, anti-4-1BB, or a combination of anti-CD28 and anti-4-1BB antibodies. CD8+ T cells specific for CMV (n = 10), EBV (n = 5), or AdV (n = 3) were generated with control, anti-CD28, anti-4-1BB, or a combination of anti-CD28 and anti-4-1BB antibodies. After 13 days of culture, the cells were collected, counted, and analyzed using flow cytometry. A, Representative flow plots of the postculture cells showing the phenotypes of the CD8+ tetramer+ cells. B–D, Frequencies of central memory phenotype (B), CD28+ (C), and CD27+ (D) cells among CD8+ tetramer+ cells. Actual values (upper panel) and the ratio of actual values for the indicated culture conditions to those for control (lower panel) are shown for each measure. Horizontal lines in the upper panels mark the mean values. Means and SEMs are shown in the lower panels (NS, not significant, repeated measures 1-way analysis of variance). B–D, Show data pooled from at least 18 independent experiments with 17 (B) or 18 (C, D) different virus-specific CD8+ T-cell responses.

a combination of anti-CD28 and anti-4-1BB antibodies. The frequencies and numbers of CD8+ tetramer+ cells that were generated with anti-4-1BB antibody were significantly higher than those generated with control or anti-CD28 antibody (Figs. 2A–C). The number of CD8+ tetramer+ cells generated with anti-4-1BB antibody was on an average 7.9 times higher than that generated with control antibody ($P < 0.001$) (Fig. 2C). In contrast, the combination of anti-CD28 and anti-4-1BB antibodies did not result in an increased frequency or number of CD8+ tetramer+ cells compared with anti-4-1BB antibody alone (Figs. 2B, C). Importantly, the positive effect of anti-4-1BB antibody was observed regardless of the epitopes of the VSTs (Fig. 2D).

Effect of Anti-CD28 and Anti-4-1BB Antibodies on the Phenotype of the Generated Virus-specific CD8+ T Cells

Previous studies have shown that extensive ex vivo expansion of T cells may reduce the in vivo activity of adoptively transferred T cells.[23,24] We therefore evaluated the effect of anti-CD28 and anti-4-1BB antibodies on the phenotype of the generated VSTs. Most of the generated CD8+ tetramer+ cells exhibited either a central memory (CM) (CD62L+CD45RA−) or effector memory (CD62L−CD45RA−) phenotype (Fig. 3A). The proportion of cells with a CM phenotype, which persist longer and are more effective in vivo after adoptive transfer,[25] among the CD8+ tetramer+ cells did not differ with the type of

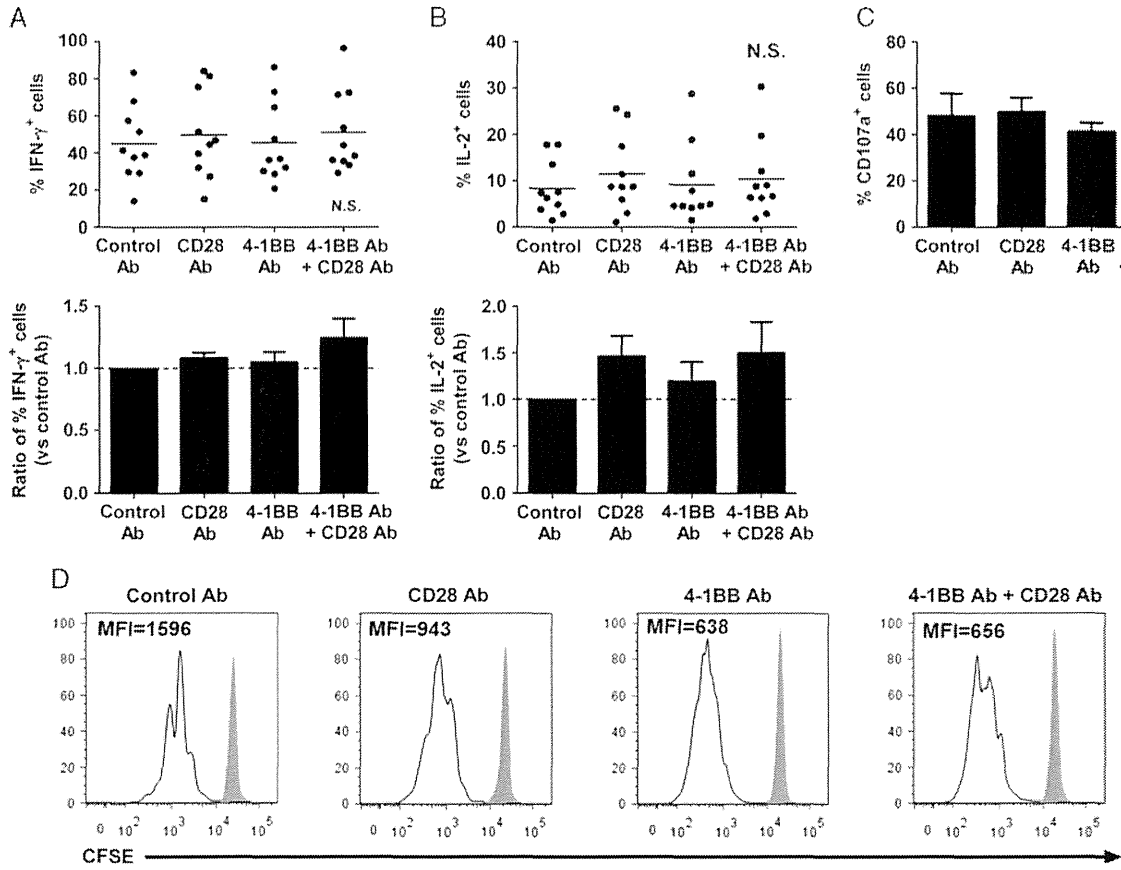

FIGURE 4. Function of virus-specific CD8+ T cells generated with control, anti-CD28, anti-4-1BB, or a combination of anti-CD28 and anti-4-1BB antibodies. A–C, Virus-specific CD8+ T cells generated with control, anti-CD28, anti-4-1BB, or a combination of anti-CD28 and anti-4-1BB antibodies were restimulated with APCs loaded with or without the corresponding peptides. After incubation, the cells were collected and analyzed for cytokine production and CD107a degranulation, as described in the Materials and methods section. Frequencies of interferon (IFN)-γ+ (A), interleukin (IL)-2+ (B), and CD107a+ (C) cells among CD8+ tetramer+ cells are shown. A and B show data pooled from at least 10 independent experiments with 10 different virus-specific CD8+ T-cell responses. Actual values (upper panel) and the ratio of actual values for the indicated culture conditions to those for control (lower panel) are shown for each measure. Horizontal lines in the upper panels mark the mean values. Means and SEMs are shown in the lower panels [NS, not significant, repeated measures 1-way analysis of variance (ANOVA)]. C, Representative data from 6 independent experiments with 3 different virus-specific CD8+ T-cell responses. Mean ± SD of triplicate wells are shown (NS, not significant, ordinary 1-way ANOVA). D, Generated virus-specific CD8+ T cells were labeled with carboxyfluorescein succinimidyl ester (CFSE), restimulated with irradiated autologous peripheral blood mononuclear cells loaded with the corresponding peptides, and analyzed for CFSE dilution using flow cytometry 120 hours after restimulation. Representative flow plots gated on CD8+ tetramer+ cells are shown. The numbers in the histograms indicate the CFSE mean fluorescence intensities (MFIs) of CD8+ tetramer+ cells. Gray shaded histograms indicate CD8+ tetramer+ cells cultured with medium alone. Data are representative of 6 independent experiments with 6 different virus-specific CD8+ T-cell responses.

antibody used. The mean percentage of cells with a CM phenotype was approximately 35% irrespective of the antibody used (Fig. 3B). Similarly, the proportion of CD28+ and CD27+ cells, which are also associated with superior in vivo efficacy after adoptive transfer,[26,27] among the CD8+ tetramer+ cells did not differ with the type of antibody used. The mean percentage of CD28+ and CD27+ cells was approximately 80% and 60%, respectively, irrespective of the antibody used (Figs. 3C, D).

Effect of Anti-CD28 and Anti-4-1BB Antibodies on the Generated Virus-specific CD8+ T-cell Function

To compare the effector functions of the generated virus-specific CD8+ T cells, cytokine production and cytotoxic activity[28] in response to the viral peptide-pulsed target cells were assessed. Virus-specific CD8+ T cells that were generated in the presence of control, anti-CD28, anti-4-1BB, or a combination of anti-CD28 and anti-4-1BB antibodies showed similar levels of IFN-γ production, IL-2 production, and CD107a expression in response to the peptide stimulation (Figs. 4A–C). In addition, the proliferative capacity of the generated virus-specific CD8+ T cells in response to the viral peptide-pulsed target cells was assessed. Of note, proliferation of the anti-4-1BB Ab-treated cells was greater than that of the control antibody treated cells, as indicated by the lower mean fluorescence intensity value in CFSE proliferation assays (Fig. 4D). The combined results indicate that anti-4-1BB antibody promotes the expansion of VSTs without causing excessive differentiation or functional deterioration of the generated T cells.

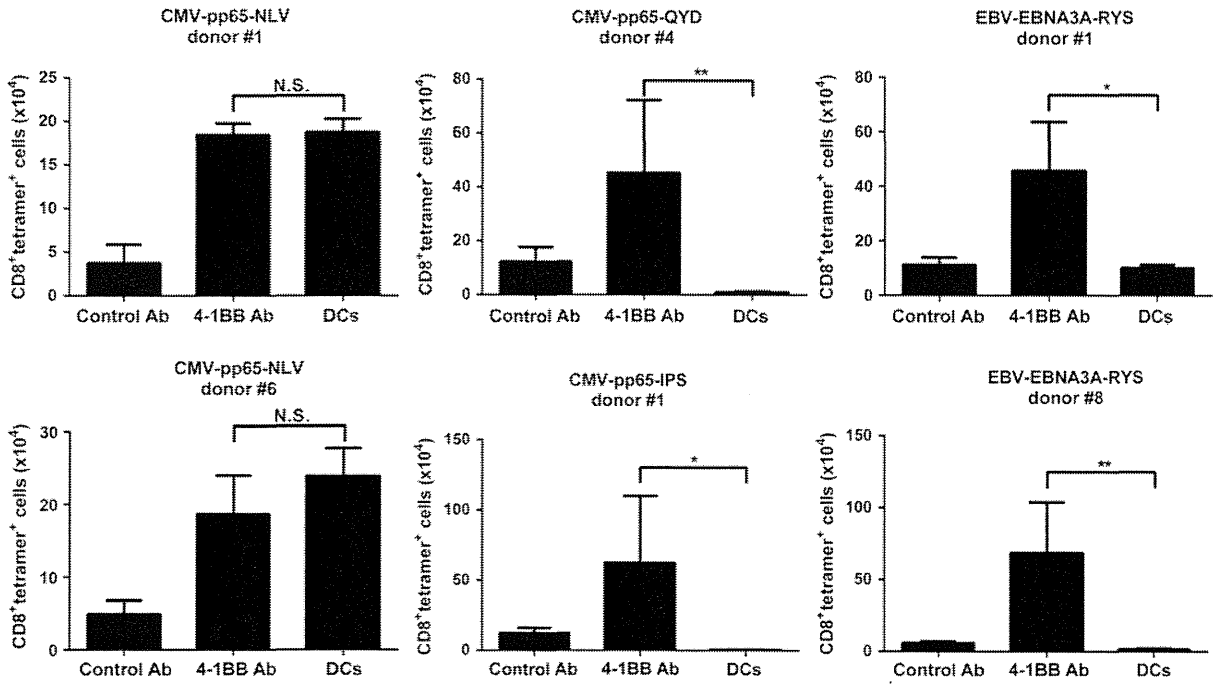

FIGURE 5. Absolute numbers of virus-specific CD8+ T cells generated with control antibody, anti-4-1BB antibody, or autologous dendritic cells (DCs). CD8+ T cells specific for CMV-pp65-QYD (n = 3), CMV-pp65-NLV (n = 2), CMV-pp65-IPS (n = 1), or EBV-EBNA3A-RYS (n = 2) epitopes were generated either with control antibody, anti-4-1BB antibody, or irradiated autologous DCs. After 13 days of culture, absolute numbers of CD8+ tetramer+ cells were determined. The means ± SD of at least triplicate wells are shown (*P < 0.05, **P < 0.01, NS, not significant, ordinary 1-way analysis of variance followed by the Tukey multiple comparison tests. Differences are shown only between anti-4-1BB antibody and DCs). Data are representative of at least 8 independent experiments with 8 different virus-specific CD8+ T-cell responses.

Comparison of Anti-4-1BB Antibody and DCs for Virus-specific CD8+ T-cell Generation

DCs are the most powerful APCs[29] and are widely used for the generation of antigen-specific T cells for adoptive immunotherapy.[9,11] To compare anti-4-1BB antibody and DCs in terms of their capacity to generate virus-specific CD8+ T cells, CD8+ T cells specific for CMV-pp65-QYD (n = 3), CMV-pp65-NLV (n = 2), CMV-pp65-IPS (n = 1), or EBV-EBNA3A-RYS (n = 2) epitopes were generated either with control antibody, anti-4-1BB antibody, or irradiated autologous DCs. The generated DCs consistently exhibited a mature phenotype (data not shown). Of note, the capacity of the DCs to generate VSTs differed considerably depending on the epitopes of the VSTs. The number of CMV-pp65-NLV-specific CD8+ T cells generated with anti-4-1BB antibody was similar to that generated with DCs. In contrast, the number of CMV-pp65-QYD-specific, CMV-pp65-IPS-specific, or EBV-EBNA3A-RYS-specific CD8+ T cells that was generated with anti-4-1BB antibody was significantly higher than that generated with DCs (Fig. 5). The phenotypes and functions of CD8+ tetramer+ cells generated with anti-4-1BB antibody were similar or superior to those generated with DCs (data not shown). These results indicate that anti-4-1BB antibody generated comparable or higher numbers of VSTs compared with DCs without causing excessive differentiation or functional deterioration of the generated T cells.

DISCUSSION

We demonstrated that VSTs can be generated rapidly and efficiently by simply stimulating PBMCs with peptide and anti-4-1BB antibody without using APCs. As there are 2 clinical grade anti-4-1BB antibodies (BMS-663513 and PF-05082566),[15,30] this method can be readily tested in clinical trials. We propose using anti-4-1BB antibody as a novel strategy to generate VSTs for adoptive therapy.

It has been reported that DCs (cytokine-activated monocytes) have only a limited capacity for generation of cytotoxic T-cell responses to subdominant epitopes.[10,31] In line with these studies, in the present study the number of VSTs generated with DCs was similar to the number generated with anti-4-1BB antibody for CMV-pp65-NLV-specific CD8+ T cells, whose epitope is generally regarded as an immunodominant epitope,[10] but the number of DC-generated VSTs specific for other epitopes was lower (Fig. 5). These results suggest that DCs may be suboptimal for the generation of VSTs that are specific for subdominant epitopes. In contrast, anti-4-1BB antibody promoted the generation of VSTs irrespective of the epitope of the VST (Fig. 2D). Therefore, anti-4-1BB antibody may be used to promote the generation of VSTs for both dominant and subdominant epitopes.

Previous studies that compared the functions of purified T cells that received TCR stimulation alone and those that received TCR and 4-1BB stimulation showed that 4-1BB stimulation improved the effector function of T cells.[5,32,33] In contrast, we did not find significant differences between the effector function of VSTs generated with anti-4-1BB antibody and those generated with control antibody. As PBMCs contain B cells and monocytes, which have the capacity to function as APCs, these cells might have provided some costimulatory signals to VSTs, resulting in similar effector functions to the control cells.

Although VSTs generated with the anti-4-1BB antibody showed similar phenotypes and effector functions to those generated with control antibody, the former had improved proliferative capacity (Fig. 4D). Thus, the results of the current study suggest that anti-4-1BB antibody, at the least, does not lead to deterioration of the function of the generated VSTs.

In the current study, anti-4-1BB antibody was more potent than anti-CD28 antibody in expanding VSTs, which was in accordance with the results of previous studies that evaluated the effect of costimulatory signals on T-cell expansion using artificial APCs expressing costimulatory molecules.[7,32] This result could be explained by the fact that CD28 costimulation preferentially expands naive T cells, whereas 4-1BB costimulation preferentially expands memory T cells.[32] In addition, the combination of anti-4-1BB and anti-CD28 antibodies did not show additive or synergistic effects compared with anti-4-1BB antibody alone. A previous study reported that additive effects of 4-1BB and CD28 dual costimulation on T-cell expansion were observed only when IFN-γ in the culture medium was neutralized.[6] Therefore, an antibody cocktail consisting of anti-4-1BB, anti-CD28, and IFN-γ neutralizing antibodies may further enhance the expansion of VSTs. Alternatively, a combination of anti-4-1BB and anti-OX40 antibodies may further promote the generation of VSTs.[7] The optimal combination of antibodies for the generation of VSTs remains to be determined.

Overlapping peptide pools that span the complete sequence of viral proteins are becoming more widely used to generate VSTs because VSTs specific for both known and unknown epitopes can be generated.[11,34] Another advantage of overlapping peptide pools is that both $CD4^+$ and $CD8^+$ VSTs can be generated,[11] which may promote the survival and persistence of the generated T cells after adoptive transfer.[35] As in the current study we stimulated PBMCs with viral-specific $CD8^+$ T-cell epitope peptides, the effect of anti-4-1BB antibody on the generation of viral-specific $CD4^+$ T cells was not examined. In this regard, some studies have shown that 4-1BB stimulation activates $CD4^+$ T cells and $CD8^+$ T cells to a similar extent,[22,36] whereas others have suggested that 4-1BB stimulation preferentially activates $CD8^+$ T cells over $CD4^+$ T cells.[33,37] Whether anti-4-1BB antibody can improve the generation of not only $CD8^+$ VSTs but also of $CD4^+$ VSTs from PBMCs stimulated with overlapping peptide pools needs to be investigated in future studies.

In conclusion, we have clearly demonstrated that VSTs can be generated rapidly and efficiently by simply stimulating PBMCs with viral peptide and anti-4-1BB antibody without using APCs. We propose using anti-4-1BB antibody as a novel strategy to generate VSTs for adoptive therapy.

CONFLICTS OF INTEREST/ FINANCIAL DISCLOSURES

This work was supported by the Japan Society for the Promotion of Science (JSPS) (25-3298 to N.I.), the Hori Sciences and Arts Foundation (N.I.), and JSPS KAKENHI (Grant-in-Aid for Scientific Research (C) 25461446 to T.N.). H.K.: Research funding from Bristol-Myers Squibb, Chugai Pharmaceutical Co. Ltd, Kyowa Hakko Kirin Co. Ltd, Dainippon Sumitomo Pharma, Zenyaku Kogyo, and FUJIFILM Corporation. T.N.: Research funding was from Bristol-Myers Squibb, Chugai Pharmaceutical Co. Ltd, Kyowa Hakko Kirin Co. Ltd, Dainippon Sumitomo Pharma, Zenyaku Kogyo, FUJIFILM Corporation, Nippon Boehringer-Ingelheim Co. Ltd, Otsuka Pharmaceutical Co. Ltd, and Toyama Chemical Co. Ltd.

The remaining authors have declared there are no financial conflicts of interest with regard to this work.

REFERENCES

1. Anderson EJ. Viral diagnostics and antiviral therapy in hematopoietic stem cell transplantation. *Curr Pharm Des.* 2008;14:1997–2010.
2. Tormo N, Solano C, Benet I, et al. Lack of prompt expansion of cytomegalovirus pp65 and IE-1-specific IFNgamma CD8 + and CD4 + T cells is associated with rising levels of pp65 antigenemia and DNAemia during pre-emptive therapy in allogeneic hematopoietic stem cell transplant recipients. *Bone Marrow Transplant.* 2010;45:543–549.
3. Leen AM, Bollard CM, Mendizabal AM, et al. Multicenter study of banked third-party virus-specific T cells to treat severe viral infections after hematopoietic stem cell transplantation. *Blood.* 2013;121:5113–5123.
4. Barker JN, Doubrovina E, Sauter C, et al. Successful treatment of EBV-associated posttransplantation lymphoma after cord blood transplantation using third-party EBV-specific cytotoxic T lymphocytes. *Blood.* 2010;116:5045–5049.
5. Bukczynski J, Wen T, Ellefsen K, et al. Costimulatory ligand 4-1BBL (CD137L) as an efficient adjuvant for human antiviral cytotoxic T cell responses. *Proc Natl Acad Sci USA.* 2004; 101:1291–1296.
6. Bukczynski J, Wen T, Wang C, et al. Enhancement of HIV-specific CD8 T cell responses by dual costimulation with CD80 and CD137L. *J Immunol.* 2005;175:6378–6389.
7. Serghides L, Bukczynski J, Wen T, et al. Evaluation of OX40 ligand as a costimulator of human antiviral memory CD8 T cell responses: comparison with B7.1 and 4-1BBL. *J Immunol.* 2005;175:6368–6377.
8. Gerdemann U, Christin AS, Vera JF, et al. Nucleofection of DCs to generate Multivirus-specific T cells for prevention or treatment of viral infections in the immunocompromised host. *Mol Ther.* 2009;17:1616–1625.
9. Micklethwaite KP, Savoldo B, Hanley PJ, et al. Derivation of human T lymphocytes from cord blood and peripheral blood with antiviral and antileukemic specificity from a single culture as protection against infection and relapse after stem cell transplantation. *Blood.* 2010;115:2695–2703.
10. Hasan AN, Kollen WJ, Trivedi D, et al. A panel of artificial APCs expressing prevalent HLA alleles permits generation of cytotoxic T cells specific for both dominant and subdominant viral epitopes for adoptive therapy. *J Immunol.* 2009;183:2837–2850.
11. Gerdemann U, Keirnan JM, Katari UL, et al. Rapidly generated multivirus-specific cytotoxic T lymphocytes for the prophylaxis and treatment of viral infections. *Mol Ther.* 2012;20:1622–1632.
12. Fleischer J, Soeth E, Reiling N, et al. Differential expression and function of CD80 (B7-1) and CD86 (B7-2) on human peripheral blood monocytes. *Immunology.* 1996;89:592–598.
13. Kinnear G, Jones ND, Wood KJ. Costimulation blockade: current perspectives and implications for therapy. *Transplantation.* 2013;95:527–535.
14. Melero I, Hervas-Stubbs S, Glennie M, et al. Immunostimulatory monoclonal antibodies for cancer therapy. *Nat Rev Cancer.* 2007;7:95–106.
15. Li SY, Liu Y. Immunotherapy of melanoma with the immune costimulatory monoclonal antibodies targeting CD137. *Clin Pharmacol.* 2013;5:47–53.
16. Leen AM, Sili U, Vanin EF, et al. Conserved CTL epitopes on the adenovirus hexon protein expand subgroup cross-reactive and subgroup-specific CD8 + T cells. *Blood.* 2004;104:2432–2440.
17. Terakura S, Yamamoto TN, Gardner RA, et al. Generation of CD19-chimeric antigen receptor modified CD8 + T cells

derived from virus-specific central memory T cells. *Blood.* 2012;119:72–82.
18. Bohnenkamp HR, Noll T. Development of a standardized protocol for reproducible generation of matured monocyte-derived dendritic cells suitable for clinical application. *Cytotechnology.* 2003;42:121–131.
19. Lim JB, Provenzano M, Kwon OH, et al. Identification of HLA-A33-restricted CMV pp65 epitopes as common targets for CD8(+) CMV-specific cytotoxic T lymphocytes. *Exp Hematol.* 2006;34:296–307.
20. Imahashi N, Nishida T, Ito Y, et al. Identification of a novel HLA-A*24:02-restricted adenovirus serotype 11-specific CD8 + T-cell epitope for adoptive immunotherapy. *Mol Immunol.* 2013;56:399–405.
21. Wolfl M, Kuball J, Ho WY, et al. Activation-induced expression of CD137 permits detection, isolation, and expansion of the full repertoire of CD8 + T cells responding to antigen without requiring knowledge of epitope specificities. *Blood.* 2007;110:201–210.
22. Wen T, Bukczynski J, Watts TH. 4-1BB ligand-mediated costimulation of human T cells induces CD4 and CD8 T cell expansion, cytokine production, and the development of cytolytic effector function. *J Immunol.* 2002;168:4897–4906.
23. Tran KQ, Zhou J, Durflinger KH, et al. Minimally cultured tumor-infiltrating lymphocytes display optimal characteristics for adoptive cell therapy. *J Immunother.* 2008;31:742–751.
24. Itzhaki O, Hovav E, Ziporen Y, et al. Establishment and large-scale expansion of minimally cultured "young" tumor infiltrating lymphocytes for adoptive transfer therapy. *J Immunother.* 2011;34:212–220.
25. Berger C, Jensen MC, Lansdorp PM, et al. Adoptive transfer of effector CD8 + T cells derived from central memory cells establishes persistent T cell memory in primates. *J Clin Invest.* 2008;118:294–305.
26. Zhou J, Shen X, Huang J, et al. Telomere length of transferred lymphocytes correlates with in vivo persistence and tumor regression in melanoma patients receiving cell transfer therapy. *J Immunol.* 2005;175:7046–7052.
27. Huang J, Kerstann KW, Ahmadzadeh M, et al. Modulation by IL-2 of CD70 and CD27 expression on CD8 + T cells: importance for the therapeutic effectiveness of cell transfer immunotherapy. *J Immunol.* 2006;176:7726–7735.
28. Rubio V, Stuge TB, Singh N, et al. Ex vivo identification, isolation and analysis of tumor-cytolytic T cells. *Nat Med.* 2003;9:1377–1382.
29. Banchereau J, Steinman RM. Dendritic cells and the control of immunity. *Nature.* 1998;392:245–252.
30. Fisher TS, Kamperschroer C, Oliphant T, et al. Targeting of 4-1BB by monoclonal antibody PF-05082566 enhances T-cell function and promotes anti-tumor activity. *Cancer Immunol Immunother.* 2012;61:1721–1733.
31. Trivedi D, Williams RY, O'Reilly RJ, et al. Generation of CMV-specific T lymphocytes using protein-spanning pools of pp65-derived overlapping pentadecapeptides for adoptive immunotherapy. *Blood.* 2005;105:2793–2801.
32. Zhang H, Snyder KM, Suhoski MM, et al. 4-1BB is superior to CD28 costimulation for generating CD8 + cytotoxic lymphocytes for adoptive immunotherapy. *J Immunol.* 2007;179:4910–4918.
33. Chacon JA, Wu RC, Sukhumalchandra P, et al. Co-stimulation through 4-1BB/CD137 improves the expansion and function of CD8(+) melanoma tumor-infiltrating lymphocytes for adoptive T-cell therapy. *PLoS One.* 2013;8:e60031.
34. Lugthart G, Albon SJ, Ricciardelli I, et al. Simultaneous generation of multivirus-specific and regulatory T cells for adoptive immunotherapy. *J Immunother.* 2012;35:42–53.
35. Walter EA, Greenberg PD, Gilbert MJ, et al. Reconstitution of cellular immunity against cytomegalovirus in recipients of allogeneic bone marrow by transfer of T-cell clones from the donor. *N Engl J Med.* 1995;333:1038–1044.
36. Cannons JL, Lau P, Ghumman B, et al. 4-1BB ligand induces cell division, sustains survival, and enhances effector function of CD4 and CD8 T cells with similar efficacy. *J Immunol.* 2001;167:1313–1324.
37. Shuford WW, Klussman K, Tritchler DD, et al. 4-1BB costimulatory signals preferentially induce CD8 + T cell proliferation and lead to the amplification in vivo of cytotoxic T cell responses. *J Exp Med.* 1997;186:47–55.

ublished December 17, 2014, doi:10.4049/jimmunol.1402346

Target Antigen Density Governs the Efficacy of Anti–CD20-CD28-CD3 ζ Chimeric Antigen Receptor–Modified Effector CD8$^+$ T Cells

Keisuke Watanabe,*,[1] Seitaro Terakura,*,[1] Anton C. Martens,[†,‡] Tom van Meerten,[§] Susumu Uchiyama,[¶] Misa Imai,[‖] Reona Sakemura,* Tatsunori Goto,* Ryo Hanajiri,* Nobuhiko Imahashi,* Kazuyuki Shimada,*,[#] Akihiro Tomita,* Hitoshi Kiyoi,* Tetsuya Nishida,* Tomoki Naoe,*,** and Makoto Murata*

The effectiveness of chimeric Ag receptor (CAR)–transduced T (CAR-T) cells has been attributed to supraphysiological signaling through CARs. Second- and later-generation CARs simultaneously transmit costimulatory signals with CD3ζ signals upon ligation, but may lead to severe adverse effects owing to the recognition of minimal Ag expression outside the target tumor. Currently, the threshold target Ag density for CAR-T cell lysis and further activation, including cytokine production, has not yet been investigated in detail. Therefore, we determined the threshold target Ag density required to induce CAR-T cell responses using novel anti-CD20 CAR-T cells with a CD28 intracellular domain and a CD20-transduced CEM cell model. The newly developed CD20CAR–T cells demonstrated Ag-specific lysis and cytokine secretion, which was a reasonable level as a second-generation CAR. For lytic activity, the threshold Ag density was determined to be ~200 molecules per target cell, whereas the Ag density required for cytokine production of CAR-T cells was ~10-fold higher, at a few thousand per target cell. CD20CAR–T cells responded efficiently to CD20-downregulated lymphoma and leukemia targets, including rituximab- or ofatumumab-refractory primary chronic lymphocytic leukemia cells. Despite the potential influence of the structure, localization, and binding affinity of the CAR/Ag, the threshold determined may be used for target Ag selection. An Ag density below the threshold may not result in adverse effects, whereas that above the threshold may be sufficient for practical effectiveness. CD20CAR–T cells also demonstrated significant lytic activity against CD20-downregulated tumor cells and may exhibit effectiveness for CD20-positive lymphoid malignancies. *The Journal of Immunology*, **2015, 194: 000–000.**

Chimeric Ag receptor (CAR)–transduced T (CAR-T) cell therapy is an emerging therapeutic strategy for refractory acute lymphoblastic leukemia (ALL) and chronic lymphocytic leukemia (CLL) (1, 2). Second- and later-generation CARs generally consist of a single-chain variable fragment (scFv) from a mAb fused to the signaling domain of CD3ζ, and contain one or two costimulatory endodomains, respectively (3–5). This technology has two main potential benefits over TCR gene insertion. One is that Ag recognition by CAR is independent of HLA, meaning that CAR therapy can be used to treat all Ag-positive patients regardless of their HLA. The other is that once CARs ligate to target molecules, full activation signals, including costimuli such as CD28 or 4-1BB, are transmitted to CAR-T cells (3–5). A superior effector function and proliferation following activation have been reported in second- and third-generation CAR-T cells (6–9).

In contrast, CAR-T cells may induce adverse effects by recognizing low expression levels of the target Ag in an off-target organ. This activity has been referred to as the "on-target/off-tumor effect." A serious adverse event induced by CAR-T cells, which recognize very low expression levels of ERBB2 on lung epithelial cells, was reported with CAR therapy targeting ERBB2 based on trastuzumab (Herceptin) (10). Although ERBB2 is expressed at low levels in various normal tissues, including lung, the anti-ERBB2 humanized mAb trastuzumab has been used safely in clinical settings (11), indicating that ERBB2 expression levels on lung cells are negligible in terms of trastuzumab therapy (12). However, ERBB2–CAR-T cells induce significant Ag-specific responses against this low expression of ERBB2 (10, 11). Therefore, selection of a target Ag is critical for both efficacy and avoiding adverse effects. TCRs recognize very low numbers of peptide/HLA complexes, whereas a relatively high number of target molecules are required for mAbs to induce cytotoxic activity (13, 14). However, the range of Ag density in which CAR-T

*Department of Hematology and Oncology, Nagoya University Graduate School of Medicine, Nagoya 466-8560, Japan; [†]Department of Hematology, VU University Medical Center Amsterdam, 1007 MB Amsterdam, the Netherlands; [‡]Department of Immunology, University Medical Center Utrecht, 3508 GA Utrecht, the Netherlands; [§]Department of Hematology, University Medical Center Groningen, 9700 RB Groningen, the Netherlands; [¶]Division of Advanced Science and Biotechnology, Graduate School of Engineering, Osaka University, Osaka 565-0871, Japan; [‖]Faculty of Pharmacy, Meijo University, Nagoya 468-8503, Japan; [#]Institute for Advanced Research, Nagoya University, Nagoya 464-8601, Japan; and **National Hospital Organization Nagoya Medical Center, Nagoya 460-0001, Japan

[1]K.W. and S.T. contributed equally to this work.

Received for publication September 12, 2014. Accepted for publication November 21, 2014.

This work was supported by grants from the Foundation for Promotion of Cancer Research (Tokyo, Japan; to S.T.), the Japan Society for the Promotion of Science KAKENHI (24790969 to S.T.), the Program to Disseminate Tenure Tracking System (MEXT, Japan; to K.S.), a Grant-in-Aid for Challenging Exploratory Research (23659487 to T. Naoe), and a Health Labor Science Research Grant (H25-Immunology-104 to M.M.).

The online version of this article contains supplemental material.

Address correspondence and reprint requests to Dr. Seitaro Terakura, Department of Hematology and Oncology, Nagoya University Graduate School of Medicine, 65 Tsurumai, Showa-ku, Nagoya, Aichi 466-8560, Japan. E-mail address: tseit@med.nagoya-u.ac.jp

Abbreviations used in this article: ABC, Ab-binding capacity; ADCC, Ab-dependent cellular cytotoxicity; ALL, acute lymphoblastic leukemia; CAR, chimeric Ag receptor; CAR-T, CAR-transduced T (cell); CDC, complement-dependent cytotoxicity; CLL, chronic lymphocytic leukemia; DLBCL, diffuse large B cell lymphoma; FCM, flow cytometry; LCL, EBV-transformed lymphoblastoid cell line; MFI, mean fluorescence intensity; ofa, ofatumumab; sABC, specific Ab binding capacity; scFv, single-chain variable fragment; tEGFR, truncated version of the epidermal growth factor receptor.

www.jimmunol.org/cgi/doi/10.4049/jimmunol.1402346

cells can recognize and induce cytotoxicity has not been investigated in detail. Furthermore, research has not yet clarified the number of Ag molecules expressed that could be candidates for targets when expressed at low levels or that should be avoided owing to the on-target/off-tumor effect (15).

CD20 is an activated glycosylated phosphoprotein that is expressed on the surface of B lymphocytes. An anti-CD20 mAb is an effective therapeutic option for various B cell malignancies such as ALL (16), CLL (17), and malignant lymphoma (18, 19). Although combination chemotherapies with rituximab have achieved favorable results in CD20-positive B cell lymphoma patients, acquired resistance to rituximab has become a problem, with a suggested mechanism of reduced expression of CD20 (20–24). Accordingly, a therapeutic option that efficiently eradicates target cells expressing low levels of CD20 that survive rituximab or ofatumumab (ofa) therapy needs to be developed. Therefore, we developed a novel CD20-CAR and investigated the minimum threshold Ag expression level required for lysis of target cells and activation of CAR-T cells. To avoid possible immunological rejection against anti-mouse Abs, we used a humanized anti-CD20 mAb to construct CD20CAR (25). We also assessed its effects against tumor cell lines and primary cells isolated from mAb therapy-refractory, CD20-downregulated B cell tumors (24, 26, 27).

Materials and Methods

Cell lines

K562, CCRF-CEM, SU-DHL-4, SU-DHL-6, SU-DHL-10, Raji, RRBL1, and WILL2 cells were cultured in RPMI 1640 medium. OCI-Ly3 and OCI-Ly10 cells were kind gifts from Dr. K. Takeyama (Dana-Farber Cancer Institute, Boston, MA) and were cultured in IMDM (Sigma-Aldrich, St. Louis, MO). Each type of medium contained 10% FBS, 0.8 mM L-glutamine, and 1% penicillin-streptomycin. RRBL1 and WILL2 cells are cell lines established from a B cell lymphoma patient who exhibited CD20-negative phenotypic changes after repeated chemotherapy with rituximab (26, 27). CD20-transduced CCRF-CEM cell lines (CD20-CEMs) expressing various levels of CD20 were described elsewhere (28). CD20-transduced K562 (CD20-K562) cells were generated by retroviral transduction with the full-length CD20 molecule, as described (29).

Primary B cell tumor cells

Primary B cell tumor cells were obtained from PBMCs (CLL patient) or pleural effusion (lymphoma patient) according to protocols approved by the Institutional Review Board of Nagoya University School of Medicine, and written informed consent was obtained from each patient in accordance with the Declaration of Helsinki.

Quantification of CD20 molecules

CD20 molecules expressed on the surface of CD20-CEMs or other cell lines were quantified using quantitative immunofluorescence indirect assay (QIFIKIT; Dako, Glostrup, Denmark). Briefly, cells were stained with unlabeled anti-CD20 mouse mAb (BD Bioscience, San Jose, CA) or purified mouse IgG-κ (BioLegend, San Diego, CA) as an isotype control. The cells of interest and calibration beads from the kit were then simultaneously labeled with primary mAb, followed by FITC-conjugated goat anti-mouse secondary Ab staining. Labeled cells and calibration beads were analyzed on a flow cytometer, and a standard regression line between fluorescence intensity and Ag density that was expressed as Ab-binding capacity (ABC) in molecules per cell was calculated. Finally, the specific ABC (sABC) was determined by subtracting the background Ab equivalent of the isotype control from ABC (30).

Retroviral vector construction

CD20-binding scFv was constructed based on the reported sequences of the humanized anti-CD20 mAb (OUBM mAb) (25). OUBM mAb exhibits high CD20 binding affinity (K_D, 10.09 nM). H chain and L chain V region segments were linked with an 18-aa linker. scFv was then fused to a human IgG_4 hinge, a CD3-ζ chain, a CD28 costimulatory domain, and a truncated version of the epidermal growth factor receptor (tEGFR) that lacked epidermal growth factor binding and intracellular signaling domains downstream of the self-cleaving T2A sequence (31–33). By inserting the T2A sequence between CD20CAR and tEGFR, the two proteins were coexpressed at equimolar levels from a single transcript. Cell-surface tEGFR was detected using the biotinylated anti-EGFR mAb Erbitux (Bristol-Myers Squibb, New York, NY). The CD20CAR transgene was assembled by overlap extension PCR (34). CD20CAR was inserted into LZRS-pBMN-Z, using HindIII and NotI sites, and the CD20CAR-encoding retrovirus was produced using the Phoenix-Ampho system (Orbigen, San Diego, CA) and concentrated with Retro-X Concentrator (Clontech Laboratories, Mountain View, CA).

Generation, expansion, and selection of CD20CAR-transduced T cells

The PBMCs of a normal donor were isolated by centrifugation of whole blood using Ficoll-Paque (GE Healthcare, Wauwatosa, WI). $CD8^+$ lymphocytes were then purified with immunomagnetic beads (Miltenyi Biotec, Bergisch Gladbach, Germany), activated with anti-CD3/CD28 beads (Invitrogen, Carlsbad, CA), and transduced on day 3 after activation with the recombinant human fibronectin fragment (RetroNectin, Takara Bio, Otsu, Japan) by centrifugation at 2100 rpm for 45 min at 32°C with the retroviral supernatant (multiplicity of infection = 3). T cells were expanded in RPMI 1640 medium containing 10% human serum, 0.8 mM L-glutamine, 1% penicillin-streptomycin, and 0.5 μM 2-ME and supplemented with recombinant human IL-2 to a final concentration of 50 IU/ml. CAR-positive cells were enriched using immunomagnetic selection with biotin-conjugated anti-EGFR mAb and streptavidin beads (Miltenyi Biotec). The transduced T cells were expanded in culture by plating with γ-irradiated EBV-transformed lymphoblastoid cell line (LCL) at a T cell to LCL ratio of 1:7 and supplemented with IL-2 to 50 IU/ml (29).

Flow cytometry

All samples were analyzed with flow cytometry (FCM) on the FACSAria instrument (BD Biosciences), and data were analyzed using FlowJo software (Tree Star, Ashland, OR). Biotinylated Erbitux and streptavidin-PE were used to identify T cells that expressed tEGFR.

[^{51}Cr] release assay and coculture assay

For the [^{51}Cr] release assay, target cells were labeled for 2 h with [^{51}Cr] (PerkinElmer, Waltham, MA), washed twice, dispensed at 2×10^3 cells per well into triplicate cultures in 96-well round-bottom plates, and incubated for 4 h at 37°C with CD20CAR–T cells at various E:T ratios. Percent of specific lysis was calculated using a standard formula [(experimental − spontaneous release)/(maximum load − spontaneous release) × 100 (%)] and expressed as the mean of triplicate samples. Regarding the coculture assay, CEMs were labeled with 0.1 μM CFSE (Invitrogen), washed, and plated with CD20 CAR-T cells at a ratio of 1:1 without IL-2 supplementation. After a 72-h incubation, cells were stained with anti-CD8 mAb and analyzed with FCM. The percentages of CAR-T cells and CEMs within the live cell gates were assessed.

Intracellular cytokine staining and cytokine secretion assay

CD20CAR–T cells and K562 or CCRF-CEM cells that expressed CD20 were mixed at a 1:1 ratio in the presence of brefeldin A (Sigma-Aldrich) and then fixed and permeabilized with Cell Fixation/Permeabilization Kits (BD Biosciences) for intracellular cytokine assay. After fixation, T cells were stained with anti–IFN-γ and anti–CD8-allophycocyanin mAb (BD Biosciences). As a positive control for cytokine production, cells were stimulated with 10 ng/ml PMA and 1 μg/ml ionomycin (Sigma-Aldrich). CD20CAR–T cells and CEMs for the cytokine secretion assay were plated at an E:T ratio of 1:1, and IFN-γ, TNF-α, and IL-2 in the supernatant were measured with ELISA (BD Biosciences) after 16 h of incubation.

CFSE proliferation assay

CD20CAR–T cells were labeled with 0.2 μM CFSE, washed, and then plated with stimulator cells at a ratio of 1:1 without IL-2 supplementation. After a 72- or 96-h incubation, cells were stained with the anti-CD8 mAb, samples were analyzed with FCM, and the division of live $CD8^+$ T cells was assessed with CFSE dye dilution.

Intracellular phospho-flow analysis

CD20CAR–T cells and CD20-CEM cells expressing various levels of CD20 were mixed at a 1:5 ratio, centrifuged briefly, and incubated for various times at 37°C. Cells were then fixed by the addition of BD Cytofix Fixation Buffer at 37°C for 10 min, permeabilized in ice-cold BD Phosflow Perm Buffer III, and incubated on ice for 30 min (BD Biosciences). P-p44/42 MAPK (T202/Y204) or P-Zap-70 (Y319)/SyK(Y532) Rabbit Ab (Cell

Signaling Technology, Danvers, MA) and bovine anti-rabbit IgG-FITC as a secondary Ab (Santa Cruz Biotechnology, Dallas, TX) were used for phospho-specific staining.

Statistical analysis

Differences among results were evaluated with one-way or two-way ANOVA analysis and the Bonferroni test, as appropriate. Differences were considered significant when $p < 0.05$. Statistical analysis was performed using GraphPad Prism Version 5 software.

Results

Generation and functional analysis of CD20CAR-transduced T cells

To develop functional CD20CAR, we constructed CD20CAR consisting of anti–CD20-scFv linked to CD3ζ, a CD28 costimulatory domain, and a tEGFR; $CD8^+$ T cells were then retrovirally transduced with CD20CAR (Fig. 1A). After one course of stimulation and transduction, the expression of CD20CAR generally reached 40–80%. To determine transduction efficiency, CD20CAR and tEGFR were labeled with an anti-Fc Ab and biotinylated Erbitux, respectively. The expression of tEGFR reflected that of CAR on the transduced T cells, and we verified that the expression of CAR and tEGFR was similar after each transduction experiment (Fig. 1B) (32). Transduction efficiency could be monitored with tEGFR with high reproducibility (Fig. 1B, *right panel*). Using intracellular staining, we assessed the ability of CAR-T cells to produce IFN-γ in response to CD20. Stimulation with CD20-K562 cells induced robust production of IFN-γ, whereas mock-transduced K562 cells did not (Fig. 1C). These results demonstrated that CD20CAR–T cells recognized CD20 in an Ag-specific manner. After the transduction culture, CD20CAR-positive cells were enriched to a purity of >95% with biotinylated Erbitux and anti-biotin immunomagnetic beads (32), expanded by stimulating with a γ-irradiated LCL, and then used for subsequent experiments. The expression of CAR/tEGFR before and after LCL stimulation was sufficiently maintained (Fig. 1D). The ability of CD20CAR–T cells to lyse $CD20^+$ target cells was assessed after one course of transduction and expansion. CD20CAR–T cells specifically lysed CD20-K562 cells (Fig. 1E) in a highly reproducible manner (Fig. 1E, *right panel*). To examine background cytotoxicity, CD19CAR (non–target-specific CAR)–transduced T cells were examined for cytotoxicity against K562 or CD20-K562. Both experiments demonstrated almost the same range of cytotoxicity by the CD20CAR–T cells against K562 as in Fig. 1E. The range of cytotoxicity was 7–11% at an E:T ratio of 10:1 ($n = 4$). Two repeated LCL stimulations caused a log-scale expansion that resulted in 10,000-fold expansion of CD20CAR–T cells (Supplemental Fig. 1). The CD20CAR–T cells almost uniformly demonstrated effector phenotype ($CD28^-$, $CD62L^-$, $CD45RO^+$) after LCL stimulation (data not shown). In all subsequent experiments, $CD20CAR^-$ T cells were selected with tEGFR and expanded with one course of LCL stimulation; thus the transduction level of CD20CAR was uniformly >95% (Fig. 1D).

Quantification of CD20 molecules on the surface of CD20-CEMs and cell lines

Although CAR-T cells very efficiently recognize targets, the range of target molecule expression to which CAR-T cells can respond

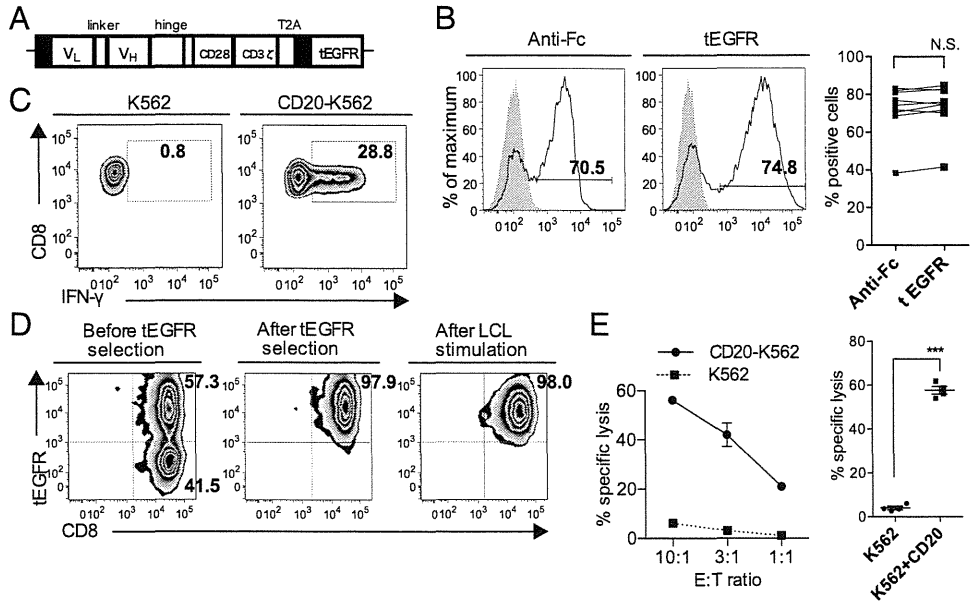

FIGURE 1. Construction, surface expression, and functional analysis of CD20CAR. (**A**) Schematic representation of the CD20CAR construct. CD20CAR consisted of anti-CD20 scFvs linked to CD3ζ, a CD28 costimulatory domain, and tEGFR as a transduction or selection marker via the T2A sequence. Solid black boxes denote the GM-CSF receptor leader sequence. Hinge, a human IgG4 hinge; linker, an 18-aa-long GGGS linker; V_H, H chain variable fragment; V_L, L chain variable fragment. (**B**) Surface expression of CD20CAR and tEGFR after transduction. $CD8^+$ cells were selected and transduced with the CD20CAR-encoding retrovirus supernatant. CD20CAR was stained with the anti-Fc Ab or biotinylated Erbitux, which reflects CAR expression. The surface expression of Fc/tEGFR was assessed on day 8 after one course of retroviral transduction. Gray-shaded histograms show staining of untransduced T cells. Representative flow plots are shown. *Right panel*, Data were pooled from nine independent experiments with T cells from eight donors (NS, paired *t* test). (**C**) Functional analysis of CD20CAR–T cells. On day 9 after transduction, CD20CAR–T cells were stimulated with either CD20-transduced K562 (CD20-K562) or mock-transduced K562 (K562) cells for 4 h at a 1:1 ratio, permeabilized, and then stained for IFN-γ. (**D**) Purity of CD20CAR–T cells before and after tEGFR selection and LCL stimulation. CD20CAR-positive cells were enriched by tEGFR selection and expanded by stimulation with γ-irradiated LCLs at a 1:7 ratio. Representative flow plots of three independent experiments from three donors are shown. (**E**) Cytotoxicity of CD20CAR–T cells. *Left panel*, After one course of expansion, cytotoxicity against either CD20-K562 or K562 cells was assessed at the indicated E:T ratio in the [^{51}Cr] release assay. The means ± SD of triplicate wells are shown. *Right panel*, Data were pooled from four independent experiments with CD20CAR–T cells from four donors (mean and SEM, ***$p < 0.0001$, the Student *t* test).

remains unknown (3–5). To assess this range more precisely, the number of CD20 molecules expressed on the cell surface of various cell lines was quantified as the CD20-specific Ab-binding capacity (CD20-sABC) on a per cell basis. We obtained 30 clones of CD20-CEMs expressing various levels of CD20 for use as target cells or stimulators (28). Of these, expression of CD20 by four representative clones was depicted, and the cells were used for several subsequent experiments as stimulators [CD20–very low CEM (VL-CEM) (CD20-mean fluorescence intensity [MFI]: 126/sABC: 240 molecules); CD20–low CEM (L-CEM) (CD20-MFI: 576/sABC: 5320 molecules); CD20–medium CEM (M-CEM) (CD20-MFI: 2396/sABC: 26,900 molecules); and CD20–high CEM (H-CEM) (CD20-MFI: 11,388/sABC: 142,722 molecules)] (Fig. 2A, Table I). The CD20-sABC values were 500,000 molecules for the germinal center B cell–type diffuse large B cell lymphoma (DLBCL)–derived cell lines; SU-DHL-4, -6, and -10, and 100,000 molecules for the non–germinal center B cell–type DLBCL-derived cell lines Ly-3 and -10 (Fig. 2B, Table I). RRBL1 and WILL2 are cell lines established from patients who experienced a relapse in B cell lymphoma with very weak expression of CD20 and who became resistant to rituximab (26, 27). The expression levels of CD20 by RRBL1 and WILL2 cells were 15,632

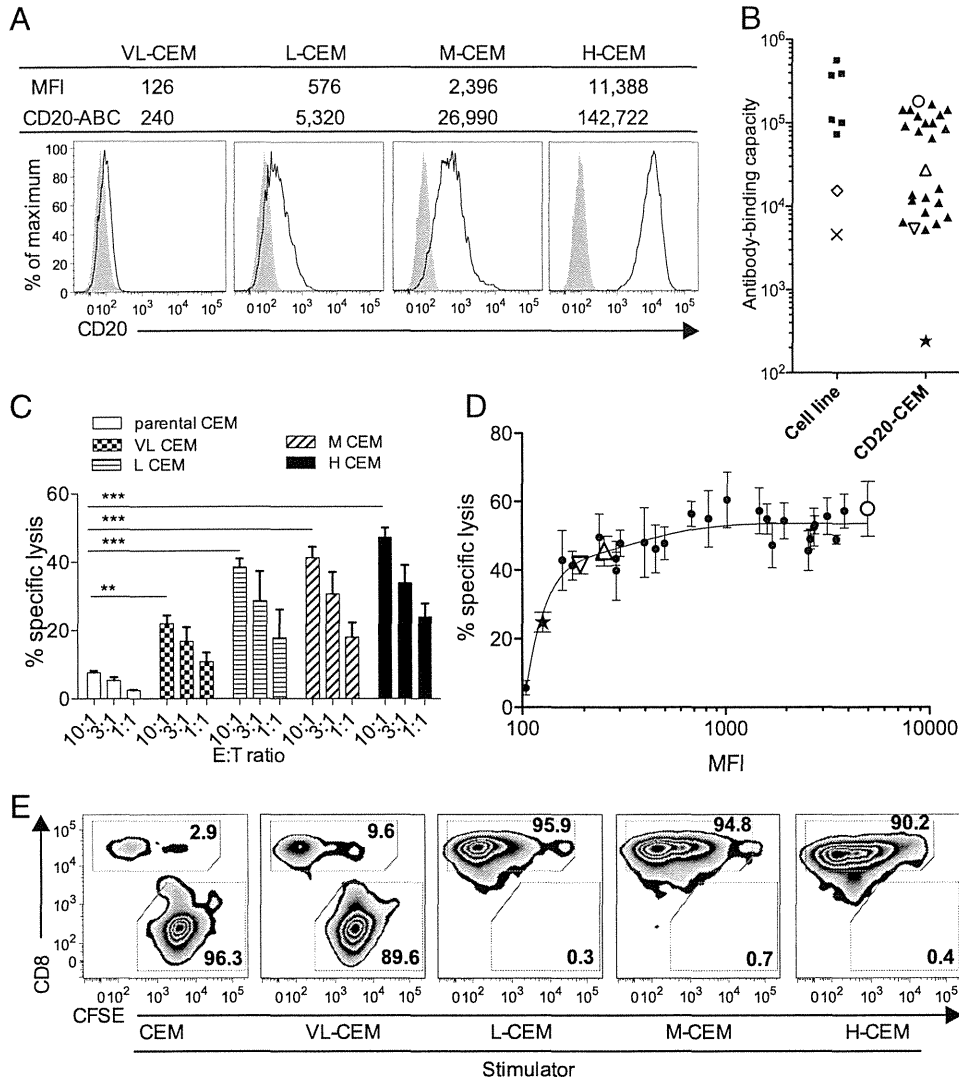

FIGURE 2. Quantification of CD20 molecules on the target cell surface and titration of the CD20 Ag expression level for CD20CAR–T cell cytotoxicity. (**A**) CD20 expression levels of the four representative CD20-CEM cell clones. The table above the histograms shows CD20-MFI and the quantification of CD20 molecules on each cell line as the Ab-binding capacity (CD20-ABC). Gray histograms show CD20 staining of untransduced CEM cells. VL-CEM, CD20-very low CEMs; L-CEM, CD20-low CEMs; M-CEM, CD20-medium CEMs; H-CEM, CD20-high CEMs. (**B**) Quantification of CD20 molecules on the surface of various cell lines. The number of CD20 molecules expressed on the surface of tumor cell lines was plotted in the left column (×, WILL2 cells; ◇, RRBL1 cells; ■, other cell lines). The number on CD20-CEMs is shown in the right column, including the four representative CEMs (★, VL-CEM; ▽, L-CEM; △, M-CEM; ○, H-CEM; ▲, other CD20-CEMs) (B, **D**). CD20-MFI data were analyzed in three independent experiments with similar results. CD20-MFI data in (A), (B), and (D) were collected in different experiments. (**C**) Cytotoxicity of CD20CAR–T cells against the four representative CD20-CEMs. Bars represent the cytotoxicity of CD20CAR–T cells against the four CD20-CEMs or untransduced CEMs (parental CEMs) at the indicated E:T ratios in the [^{51}Cr] release assay. The means ± SD of triplicate wells are shown (**$p < 0.01$, ***$p < 0.0001$, two-way ANOVA analysis). (D) The correlation between the CD20-MFI of CD20-CEMs and the cytotoxicity of CD20CAR–T cells. The cytotoxicity of CD20CAR-T cells against each CD20-CEM cell line was determined as in (C). The cytotoxicity of each CD20-CEM cell line at an E:T ratio of 10:1 was plotted against the CD20-MFI of CD20-CEMs. Data were pooled from four independent experiments with CD20CAR–T cells from four donors (mean and SEM). The solid line represents the fitted curve obtained with the nonlinear regression model using Prism5 software. (**E**) CD20CAR–T cells eradicated CD20-CEMs in coculture assays according to CD20 expression levels. CAR-T cells and CFSE-labeled CEMs were cultured in a 1:1 ratio without IL-2 supplementation for 72 h. The percentage of surviving CAR–T cells and residual CEMs within the live cell gates are shown. Data are representative of three independent experiments using three independent CD20CAR–T cell lines.

Table I. Surface CD20 expression of CD20-CEMs and other tumor cell lines

	MFI	sABC
CEM		
Parental	121	0
#2	9,683	120,208
#3	11,403	142,921
#4	6,905	83,978
#7	7,491	91,567
#19	14,228	180,597
#23	1,293	13,675
#27	11,388	142,722
#29	8,045	98,770
#31	15,550	198,366
#37	845	8,414
#47	1,209	12,680
#71	563	5172
#72	6,494	78,675
#73	8,049	98,822
#76	126	240
#82	641	6,062
#85	9,922	123,353
#94	576	5,320
w6	15,672	200,009
w7	13,180	166,571
w12	1,063	10,960
w40	5,414	64,824
w54	17,930	230,546
w114	1,125	11,689
w127	749	7,303
w132	1,497	16,104
w141	669	6,383
w147	2,396	26,990
w149	11,363	142,390
Tumor cell line		
RRBL1	1,436	15,376
WILL2	510	4,571
DHL-4	33,076	390,664
DHL-6	31,713	371,994
DHL-10	6,983	564,656
Ly-3	6,798	73,049
Ly-10	9,206	100,965
Raji	9,949	108,985

and 4869 molecules per cell, respectively (Fig. 2B, ◇ and ×, respectively). Relative to other cell lines, CD20-CEMs represented a very wide range of CD20 expression, from 240 to 230,546 molecules per cell, which was considered very low to high (Fig. 2B, Table I).

To evaluate the potential influence of costimulation, inhibitory signals, and adhesion molecule, the expression of CD80, CD86, CD54 (ICAM-1), CD58 (leukocyte function–associated molecule-3), and PD-L1 on target tumor cells was investigated. CEM cells demonstrated a tolerogenic phenotype, expressing low levels of CD80 and CD86 and relatively high levels of the inhibitory ligand PD-L1. CD54 was positive in all examined cell lines, whereas CD58 was negative in WILL2 cells (Supplemental Fig. 2) (35).

Determination of the minimum threshold of CD20 expression that CAR-T cells require for recognition and lysis

The level of CD20 Ag expression for rituximab-induced complement-dependent cytotoxicity (CDC) was determined using the same set of CD20-CEMs (28). We performed the rituximab-induced CDC assay and obtained almost the same results using human complement (Supplemental Fig. 3A). As demonstrated previously, Ab-dependent cellular cytotoxicity (ADCC) with rituximab against CD20-CEMs did not show a clear threshold of CD20 expression (data not shown) (28). CD20-CEMs with an MFI <1000 (equivalent to sABC of 10^4) did not induce significant CDC, whereas CD20-CEMs with an MFI of 1000–3000 (equivalent to sABC of 10^4–10^5) did. CD20-CEMs with an MFI >3000 effectively induced cytotoxicity, and maximal CDC was obtained at an MFI >5000 (sABC of 10^5) (Supplemental Fig. 3A). CDC induced by the humanized anti-CD20 mAb OUBM was also examined. OUBM mAb, with which CD20CAR was constructed, induced marked CDC with half-maximum cytotoxicity at a CD20 expression level similar (MFI of 3000) to that of rituximab (MFI of 3000) (Supplemental Fig. 3).

In contrast to the weak CDC caused by rituximab and OUBM mAb, CD20-CEMs were more efficiently lysed by CD20CAR–T cells, with the exception of VL-CEMs, which underwent a significantly lower degree of lysis (Fig. 2C).

To determine the threshold expression level of the CD20 Ag required to induce CAR-T cytotoxicity, we performed a [^{51}Cr] release assay with CD20CAR–T cells against the clones of CD20-CEMs expressing various levels of CD20 (CD20-MFI: 126–6924/CD20-sABC: 240–230,546 molecules). CD20CAR–T cells lysed VL-CEMs, which had the lowest level of CD20 (MFI: 126/sABC: 240 molecules, 22.8 ± 2% lysis). In addition, CD20CAR–T cells induced similar lysis (40–60% lysis) of various CD20-CEMs with higher expression of CD20 (CD20-MFI: 157/CD20-sABC: ≥5172 molecules, E:T ratio of 10:1) (Fig. 2D). CD20CAR–T cells exhibited efficient cytotoxicity against CD20-CEMs with an MFI <1000; at this level, rituximab and OUBM mAb did not induce significant CDC (Supplemental Fig. 3A, 3B, Fig. 2D). Half-maximum cytotoxicity by CD20CAR–T cells was observed at an MFI of ~200–300 (equivalent to sABC of 10^3). Therefore, the minimum threshold number of surface target molecules that CAR-T recognized and lysed was markedly low, at approximately a few hundred molecules.

A coculture assay was performed as a more physiological model. In this assay, CD20CAR–T cells partially, but not completely, eradicated VL-CEMs. Conversely, CAR-T cells completely eradicated L-, M-, and H-CEMs after a 72-h coculture (Fig. 2E).

Intracellular signaling, cytokine production, and cell division after stimulation with the four representative CD20-CEMs

An advantage of CAR-T cell therapy over mAb therapy is that CAR-T cells can become activated and proliferate upon specific stimulation of the target Ag, enabling CAR-T cells to exhibit long-lasting efficacy in vivo (1, 3–5, 9). Although we titrated the threshold Ag density for CAR-T–induced lysis, the threshold for cytotoxicity and full activation, including cytokine production and proliferation, are uncoupled in Ag-specific T cells (36). Thus, we examined the threshold Ag density for CAR-T activation. To define the minimum threshold of CD20 expression that was needed for effective activation and expansion of CAR-T cells, we examined phosphorylation of the signaling molecules ERK and ZAP70 after stimulation with the four representative CD20-CEMs. The CD20-CEMs, except for VL-CEMs, induced similar phosphorylation of ERK (pERK) and ZAP70 in CAR-T cells (Fig. 3A and data not shown). pERK was equally upregulated when CAR-T cells were stimulated with L-, M-, and H-CEMs, but not with VL-CEMs, after 10 min (Fig. 3A). Time-course analysis showed that the pERK MFI responses were almost equal after L-, M-, and H-CEM stimulation, and the peak time was 5–10 min after stimulation. Nevertheless, VL-CEM induced only minimal phosphorylation of ERK in CAR-T cells, similar to that of parental CEMs (Fig. 3A, 3B).

Cytokine production and proliferation were evaluated following different stimuli. Stimulation with VL-CEM did not induce the production of cytokines from CAR-T cells. Conversely, L-, M-, and H-CEMs induced equivalent production of IFN-γ (Fig. 3C–E), IL-2 (Fig. 3F, 3G), and TNF-α (Fig. 3H). IL-2 production after H-CEM

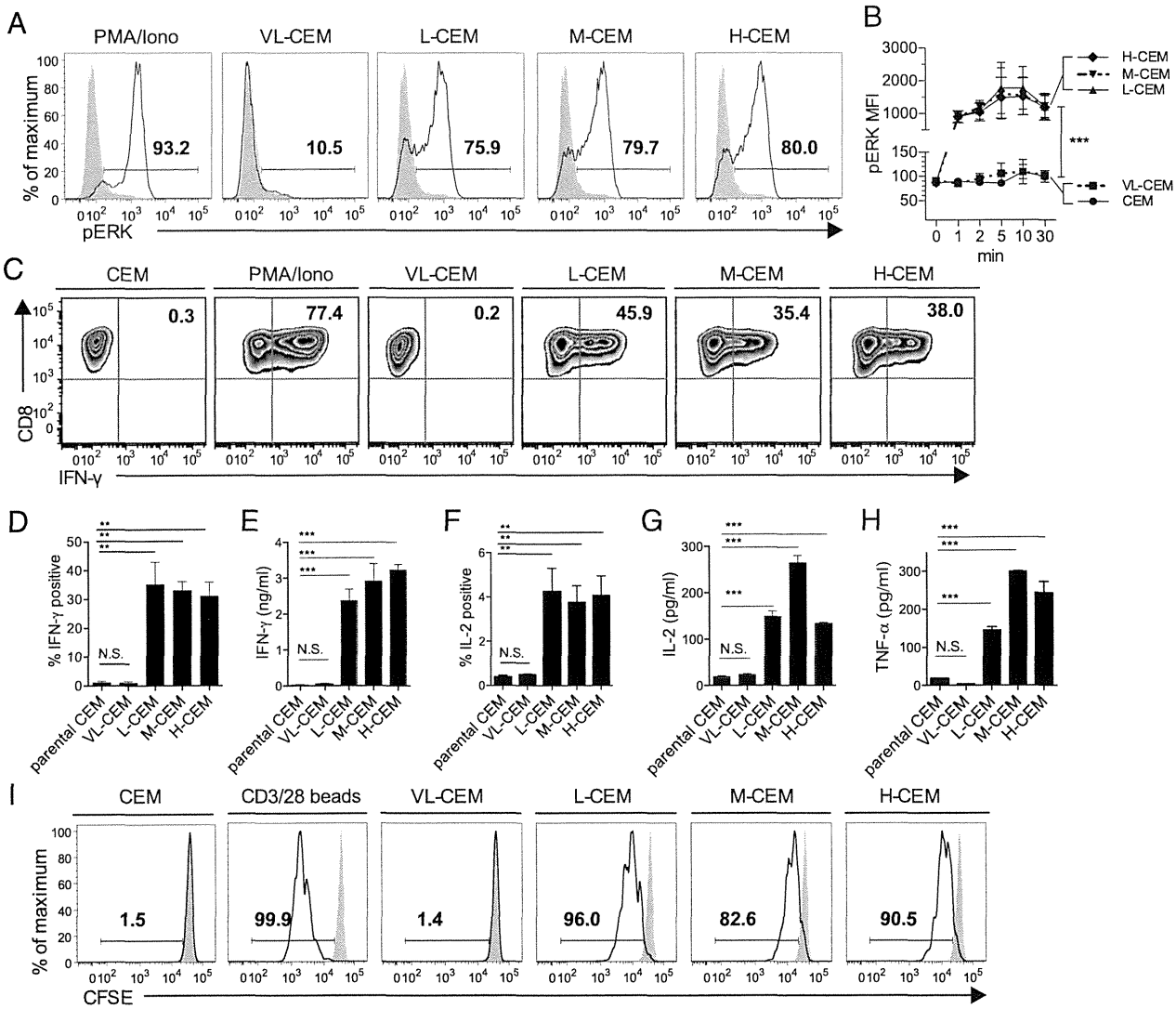

FIGURE 3. Titration of the threshold of CD20 expression for CD20CAR–T cell activation upon stimulation. (**A**) Phosphorylation of a distal signaling molecule, ERK (pERK). CD20CAR–T cells were stimulated with the four representative CD20-CEMs, untransduced CEMs at a responder to stimulator ratio of 1:5, or PMA/ionomycin (Iono) for 10 min, and were then fixed, permeabilized, and stained with pERK-specific Ab. Gray histograms show data obtained from T cells stimulated with parental CEMs. (**B**) Time-course analysis of pERK. The phosphorylation of ERK in CD20CAR–T cells was analyzed 1, 2, 5, 10, and 30 min after stimulation with the four representative CD20-CEMs or parental CEMs at a 1:5 ratio. MFI of pERK after stimulation is shown. Data were pooled from three independent experiments with CD20CAR–T cells from three donors. Means and SEM are shown (***$p < 0.0001$, two-way ANOVA analysis). (**C**) IFN-γ production after stimulation. CD20CAR–T cells were stimulated with the four representative CD20-CEMs, parental CEMs at a 1:1 ratio, or PMA/Iono for 4 h, and were then permeabilized and stained for IFN-γ. (**D** and **F**) The percentages of T cells that stained positive for IFN-γ and IL-2, respectively, are shown. Data were pooled from three independent experiments with CD20CAR–T cells from three donors (mean and SEM, **$p < 0.01$). The secretion of (**E**) IFN-γ, (**G**) IL-2, and (**H**) TNF-α upon CD20-CEM stimulation. CD20CAR–T cells were stimulated with the indicated CEMs at a 1:1 ratio, and culture supernatants were harvested at 16 h and analyzed with ELISA (mean and SEM, ***$p < 0.001$, one-way ANOVA). (**I**) Division of CD20CAR–T cells upon CD20 ligation. CD20CAR–T cells were labeled with CFSE and stimulated with CD20-CEMs, untransduced CEMs, or anti-CD3/28 beads at a 1:1 ratio, and the CFSE staining intensity was then analyzed with FCM 96 h after stimulation. Gray histograms show data of nonstimulated CD20CAR–T cells. Data are representative of at least three independent experiments with CD20CAR–T cells from three donors (A, C, and I).

stimulation was approximately half that after M-CEM stimulation in repeated experiments ($n = 3$). Because we observed no significant difference in intracellular IL-2 production (Fig. 3F), the low IL-2 concentration after H-CEM stimulation may have reflected an increase in cytokine consumption. Regarding proliferation, VL-CEM did not induce cell division of CAR-T cells, whereas other CEMs induced efficient cell division 72 and 96 h after stimulation (Fig. 3I and data not shown). The kinetics of CD20CAR–T cell division increased with higher CD20 expression on CD20-CEMs, but the percentages of proliferating cells were equivalent among L-, M-, and H-CEM stimulation (Fig. 3I). The kinetics of division appeared to be partly dependent on target Ag density (Fig. 3I).

Taken together, the minimum threshold required to induce activation and proliferation of CAR-T cells was between the levels expressed by VL-CEMs and L-CEMs. This threshold was very low: less than the CD20 expression level of L-CEMs (CD20-MFI: 576/CD20-sABC: 5320). CD20 expression above the threshold significantly activated CAR-T cells.

Effects on CD20^{lo} cell lines and CD20^{lo} primary tumor cells isolated from patients with rituximab-refractory B cell lymphoma

Because we demonstrated that CD20CAR–T cells recognized markedly low expression of CD20, we examined the effectiveness of

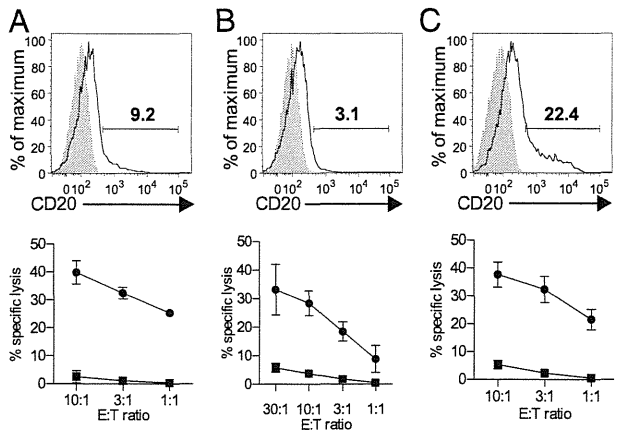

FIGURE 4. Cytotoxicity of CD20CAR–T cells against CD20-downregulated tumor cell lines and primary lymphoma cells. (**A** and **B**) CD20 expression and cytotoxicity by CD20CAR–T cells against CD20-downregulated tumor cell lines RRBL1 and WILL2, respectively. (**C**) CD20 expression and cytotoxicity by CD20CAR–T cells against primary tumor cells isolated from the pleural effusion of a patient with rituximab-refractory B cell lymphoma. Throughout the figure, *upper panels* show CD20 staining (solid line), isotype control staining (gray shaded), and percentages of CD20-positive fractions. *Lower panels* show the cytotoxicity by CD20CAR–T cells against the cell lines at the indicated E:T ratios in the [^{51}Cr] release assay. The means ± SEM of three independent experiments with CD20CAR–T cells from three donors are shown. • and ■ denote cytotoxicity by CD20CAR-T and untransduced T cells, respectively.

CD20CAR–T cell therapy against CD20^{lo} tumor cells. First, the cytotoxicity of CD20CAR–T cells against CD20^{lo} tumor cell lines was investigated. CD20CAR–T cells lysed both CD20^{lo} cell lines, RRBL1 and WILL2, very efficiently (Fig. 2B, 4A, 4B, *lower panel*).

We also evaluated cytotoxicity against CD20^{lo} primary cells from a patient with DLBCL (double-hit lymphoma). The patient exhibited disease recurrence after a full course of R-hyper CVAD (37), and lymphoma cells were obtained from pleural effusion. At the time of relapse, CD20 expression was reduced in most cells, and only ~20% of cells showed low CD20 expression (Fig. 4C, *upper panel*). CD20CAR–T cells efficiently lysed CD20^{lo} primary DLBCL cells. This lytic activity was higher than the percentage of the CD20^{+} cell fraction, suggesting that CD20CAR–T cells partially lysed the cell fraction expressing low levels of CD20 (Fig. 4C, *lower panel*).

CD20CAR–T cells recognized and lysed residual CLL cells after ofa therapy

CLL is a chronic lymphoproliferative disease in which the anti-CD20 mAb is a choice for standard care (38). The expression of CD20 by CLL cells is generally lower than that of other CD20^{+} lymphoid malignancies such as ALL and lymphoma (39). To compare the potency of CD20 recognition by anti-CD20 mAb, we examined cytotoxicity and cytokine production following stimulation of CD20-downregulated CLL cells. Before starting mAb therapy, the expression of CD20 by CLL cells was intact, and the lytic activity of CD20CAR–T cells was remarkable (Fig. 5A). The patient then became chemorefractory following repeated administration of rituximab (the clinical course of this patient is summarized in Supplemental Fig. 4). In this patient, CLL cells could not be controlled with rituximab-combined chemotherapy. The expression of CD20 by CLL cells decreased, and the MFI showed two peaks: the nearly negative fraction and the CD20 low fraction (Fig. 5B, *upper panel*). However, cytotoxicity by CD20CAR–T cells was maintained (Fig. 5B, *lower panel*). The patient was then treated with the novel anti-CD20 mAb ofa (40). A marked decrease in the number of CLL cells and regression of lymphadenopathy were observed after a single course of ofa, whereas the CD20 very low fraction, which was confirmed to consist of CD5^{+} CLL cells (data not shown), remained in the peripheral

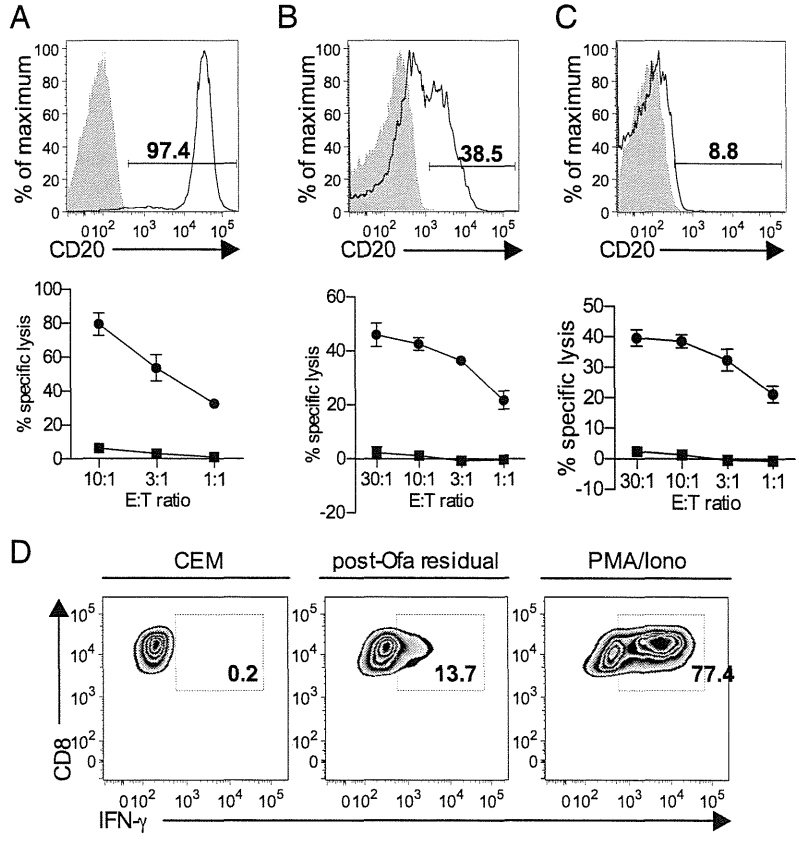

FIGURE 5. Cytotoxicity of CD20CAR–T cells against CD20-downregulated primary CLL cells. (**A–C**) CD20 expression and cytotoxicity against CLL cells isolated from an untreated patient (A), before administration of ofa (preofa) (B), and 14 d after the 10th course of ofa (postofa) (C). CLL cells were isolated from the peripheral blood of a patient with rituximab-refractory CLL. Residual CLL cells after rituximab treatment were isolated from the peripheral blood of a patient at two different time points, pre- and postofa. *Upper panels* show CD20 staining (solid line) and isotype control staining (gray shaded). *Lower panels* show cytotoxicity by CD20CAR–T cells against CLL cells at the indicated E:T ratios in the [^{51}Cr] release assay. Filled circles and squares denote cytotoxicity by CD20CAR-T and untransduced T cells, respectively. The means ± SEM of three independent experiments with CD20CAR–T cells from three donors are shown (A–C). (**D**) Cytokine production by CD20CAR–T cells upon stimulation with postofa CLL cells. CD20CAR–T cells were stimulated with postofa CLL cells, parental CEMs at a 1:1 ratio, or PMA/Iono for 4 h, and were then permeabilized and stained for IFN-γ.

blood. We obtained residual CLL cells from the peripheral blood of the patient after the 10th course of ofa. After ofa treatment, the CD20 relatively low fraction disappeared, and CD20 expression by CLL cells was almost uniformly nearly negative (Fig. 5C, *upper panel*). The residual cells were exposed once to the mAb therapy and survived. Therefore, the CD20 expression level of the residual cells was considered to be below the effective range of rituximab or ofa. In the [^{51}Cr] release assay using these primary CLL cells, CD20CAR–T cells efficiently recognized and lysed not only CLL cells before ofa but also CLL cells after ofa (Fig. 5B, 5C, *lower panel*). With an intracellular IFN-γ assay, after ofa, stimulation of CD20CAR–T cells with CLL cells, which were nearly CD20-negative, induced production of IFN-γ by CD20CAR–T cells (Fig. 5D).

Discussion

In the current study, we generated a novel CD20CAR based on a humanized anti-CD20 mAb (25). CD20CAR–T cells specifically and effectively lysed CD20-positive target cells. The expression of CD20CAR was precisely evaluated using the anti-Fc Ab and biotinylated Erbitux. Although we did not directly evaluate the copy number of the CD20CAR transgene, the variation observed in lytic activity against K562-CD20 cells was very low following tEGFR selection, suggesting that the expression of CD20CAR was similar among the CD20CAR–T cell lines. With cytotoxicity analysis of CD20CAR–T cells against CD20-CEMs expressing various levels of CD20, we first titrated the minimum threshold of CD20 expression that CAR-T cells could recognize and lyse. We demonstrated that CD20CAR–T cells lysed CD20-CEMs with CD20-ABC = 240 molecules, which was the lowest CD20 level in this set. This level was 1000-fold lower than that required to induce CDC with rituximab and OUBM mAb. The difference in cytolytic activity between CDC and CAR should mostly depend on the presence or absence of effector cells. Although CDC and CAR activity is similar against CD20-high CEM cells, CD20CAR–T cells demonstrated far better lytic activity than CDC against CD20-low CEM cells (Fig. 2D, Supplemental Fig. 3). This finding suggested that CAR-T therapy might show better effect in the case of only a limited number of target Ags on the tumor cells. The correlation between CD20-ABC and specific lysis was also represented with a saturation curve, which had a sharp inclination against CD20^{lo} targets. This phenomenon was attributed to CAR technology providing full activation with CD3ζ and the simultaneous costimulation of CD28 (3–6).

We next determined the threshold of CD20 expression that could activate and expand CD20CAR–T cells upon stimulation with the representative CD20-CEMs. Although cytotoxicity analysis revealed that CD20CAR–T cells lysed VL-CEMs, these cells did not induce downstream signaling, production of IFN-γ, or proliferation of CAR–T cells. Stimulation with L-, M-, and H-CEMs (CD20-ABC: ≥5320 molecules) effectively and equally activated CD20CAR–T cells. Taken together, these results indicated that the threshold of CD20 expression for recognition and lysis by CD20CAR–T cells, which we termed the "lytic threshold," was a few hundred molecules, and the threshold required for activation and expansion of CAR-T cells, termed the "activating threshold," was slightly higher, at a few thousand molecules. These results are consistent with previous findings in which the lytic threshold and activating threshold were different in TCR activation (36). Because endogenous T cells such as melanoma-specific T cells and virus-specific T cells require 10–100 epitope molecules per target cell to trigger specific lysis (13), both the lytic threshold and the activating threshold were slightly lower in endogenous T cells compared with CAR-T cells. Obviously, the thresholds are affected by the affinity of the mAb or TCR for the ligand or peptide/HLA complex. In our study, the affinity of the humanized anti-CD20 mAb (OUBM mAb), which was used to construct CD20CAR, was within the same range as that of rituximab (K_D value: OUBM mAb, 10.09 nM; rituximab, 5.35 nM) (25). Using a mAb with this range of affinity, both thresholds of CAR-T cells were close to those of endogenous T cells. Furthermore, CD20CAR–T cells recognized and lysed CD20-downregulated target cells that survived after mAb therapy, indicating that manufacturing a CAR with a mAb may reinforce target recognition more than the mAb itself.

The epitope location of the mAb is another important issue. Ofa exposure before sample collection may account for the apparent CD20 downregulation. However, we confirmed CD20 downregulation using another CD20 mAb, a B9E9 clone in which the epitope location is distinct from that of ofa (23). This confirmation indicated that CD20 downregulation after ofa treatment was not caused by competition between the analytical Ab and ofa. The epitope location targeted by OUBM mAb and ofa partially overlaps, but that of OUBM mAb and rituximab does not (25). Therefore, ofa can theoretically block the ligation of CD20CAR-T but rituximab cannot. We observed that CD20CAR–T cells indeed lysed CD20-downregulated target cells both after rituximab and ofa, suggesting that the potential effect of epitope blocking was minor in the current study.

The results of the current study led us to propose a novel concept for future searches for target Ag in CAR-T therapy. Suitable target Ags for CAR-T cell therapy are considerably different from those for mAb therapy in terms of their expression profiles and levels. Higher expression levels on the surface of tumor cells have been considered in target Ag searches for mAb therapy because off-tumor expression is usually negligible (41). However, for the target of CAR-T cell therapy, off-tumor expression of the target molecules must be strictly negative or at a very low level that is below the lytic threshold, at a few hundred molecules. Otherwise, severe adverse effects could occur as a result of off-tumor effects (10). The target Ag safety in the context of mAb therapy does not necessarily translate into the safety of Ag in the context of markedly more sensitive CAR-T cell therapy (10). Conversely, even if the threshold was below the mAb therapy range, low Ag expression above the activating threshold, such as at a few thousand molecules, could be considered a candidate for the target Ag of CAR-T cell therapy.

Acquired resistance to rituximab has become a problem in the treatment of patients with CD20-positive B cell tumors (20, 23). One suggested mechanism is downregulation of CD20 (20, 22, 26). A total of 15–20% of relapsed patients exhibit CD20 Ag loss, as observed with immunohistochemistry analysis in samples taken at relapse (20, 23). Our CD20CAR–T cells recognized and lysed primary cells isolated from patients with mAb therapy–refractory lymphoma and CLL, although the expression level of CD20 was very low. We also analyzed CD20CAR-T recognition against CD20-downregulated, mAb-refractory CLL in detail (21). The residual cells after CD20 mAb therapy expressed significantly low levels of CD20, and this expression level must have been below the effective range of the mAb in principle. CD20CAR–T cells lysed both postrituximab and postofa residual CLL cells, indicating that CD20CAR–T cells have a greater potential to recognize the target than mAbs. Even residual postofa CLL cells stimulated CD20CAR–T cells, and thus we conclude that the very low expression of CD20 on CLL cells could still efficiently provide stimulation for the further repopulation of CD20CAR–T cells.

In other CAR therapies targeting CD19, several patients were reported to have relapsed despite the completely negative con-

version of the Ag molecule after CAR-T cell therapy (2). Although CAR-T cells recognize very low levels of the target Ag, they cannot recognize completely Ag-negative cells. The strategy of administering CAR-T therapy as a first-line treatment, or in earlier phases with the aim of earlier eradication of target cells, may prevent immunological escape by negative conversion of the Ag.

One limitation of the current study is that we assessed the threshold using only CD20 and CD20CAR systems. Because the threshold may be influenced by many other factors, such as affinity (42), structure (43), epitope localization of individual CAR-Ag pairs (44, 45), and the expression of a coreceptor on target cells (46), the threshold may vary among mAbs and target Ags. We also could not investigate the relationship between the expression of CD20 and the ADCC activity of mAbs because NK cell activity is predominant in the CD20-CEM system, and a clear threshold has not been observed (28). Although the potential relationship between target Ag density and ADCC activity has been investigated in other experimental systems, $>10^4$ Ag molecules per cell are needed to demonstrate significant ADCC (47). In the current study, the minimum threshold of CAR recognition was 3-log units lower than that of mAbs to trigger CDC. CAR can also directly mobilize T cells to target cells, whereas mAb therapy mainly depends on indirect cytotoxicity such as CDC or ADCC (3–5, 19, 28). Thus, the lytic and activating thresholds of CAR are considered significantly lower than those of mAbs.

We concluded that CAR-T cells can recognize and lyse cells expressing considerably low levels of the target Ag and were activated and expanded upon such stimulation. CD20CAR–T cell therapy may also be applicable for the treatment of CD20-positive lymphoid malignancies.

Acknowledgments

We thank Yoko Matsuyama, Asako Watanabe, and Chika Wakamatsu for technical assistance.

Disclosures

H.K. has received research funding from Bristol-Myers Squibb, Chugai Pharmaceutical, Kyowa Hakko Kirin, Dainippon Sumitomo Pharma, Zenyaku Kogyo, and FUJIFILM. The other authors have no financial conflicts of interest.

References

1. Porter, D. L., B. L. Levine, M. Kalos, A. Bagg, and C. H. June. 2011. Chimeric antigen receptor-modified T cells in chronic lymphoid leukemia. *N. Engl. J. Med.* 365: 725–733.
2. Grupp, S. A., M. Kalos, D. Barrett, R. Aplenc, D. L. Porter, S. R. Rheingold, D. T. Teachey, A. Chew, B. Hauck, J. F. Wright, et al. 2013. Chimeric antigen receptor-modified T cells for acute lymphoid leukemia. *N. Engl. J. Med.* 368: 1509–1518.
3. Sadelain, M., R. Brentjens, and I. Riviere. 2013. The basic principles of chimeric antigen receptor design. *Cancer Discov.* 3: 388–398.
4. Jensen, M. C., and S. R. Riddell. 2014. Design and implementation of adoptive therapy with chimeric antigen receptor-modified T cells. *Immunol. Rev.* 257: 127–144.
5. Turtle, C. J., M. Hudecek, M. C. Jensen, and S. R. Riddell. 2012. Engineered T cells for anti-cancer therapy. *Curr. Opin. Immunol.* 24: 633–639.
6. Kowolik, C. M., M. S. Topp, S. Gonzalez, T. Pfeiffer, S. Olivares, N. Gonzalez, D. D. Smith, S. J. Forman, M. C. Jensen, and L. J. Cooper. 2006. CD28 costimulation provided through a CD19-specific chimeric antigen receptor enhances in vivo persistence and antitumor efficacy of adoptively transferred T cells. *Cancer Res.* 66: 10995–11004.
7. Imai, C., K. Mihara, M. Andreansky, I. C. Nicholson, C. H. Pui, T. L. Geiger, and D. Campana. 2004. Chimeric receptors with 4-1BB signaling capacity provoke potent cytotoxicity against acute lymphoblastic leukemia. *Leukemia* 18: 676–684.
8. Zhong, X. S., M. Matsushita, J. Plotkin, I. Riviere, and M. Sadelain. 2010. Chimeric antigen receptors combining 4-1BB and CD28 signaling domains augment PI3kinase/AKT/Bcl-XL activation and $CD8^+$ T cell-mediated tumor eradication. *Mol. Ther.* 18: 413–420.
9. Kochenderfer, J. N., M. E. Dudley, S. A. Feldman, W. H. Wilson, D. E. Spaner, I. Maric, M. Stetler-Stevenson, G. Q. Phan, M. S. Hughes, R. M. Sherry, et al. 2012. B-cell depletion and remissions of malignancy along with cytokine-associated toxicity in a clinical trial of anti-CD19 chimeric-antigen-receptor-transduced T cells. *Blood* 119: 2709–2720.
10. Morgan, R. A., J. C. Yang, M. Kitano, M. E. Dudley, C. M. Laurencot, and S. A. Rosenberg. 2010. Case report of a serious adverse event following the administration of T cells transduced with a chimeric antigen receptor recognizing ERBB2. *Mol. Ther.* 18: 843–851.
11. Hudis, C. A. 2007. Trastuzumab—mechanism of action and use in clinical practice. *N. Engl. J. Med.* 357: 39–51.
12. Ménard, S., P. Casalini, M. Campiglio, S. M. Pupa, and E. Tagliabue. 2004. Role of HER2/neu in tumor progression and therapy. *Cell. Mol. Life Sci.* 61: 2965–2978.
13. Purbhoo, M. A., D. H. Sutton, J. E. Brewer, R. E. Mullings, M. E. Hill, T. M. Mahon, J. Karbach, E. Jäger, B. J. Cameron, N. Lissin, et al. 2006. Quantifying and imaging NY-ESO-1/LAGE-1-derived epitopes on tumor cells using high affinity T cell receptors. *J. Immunol.* 176: 7308–7316.
14. Liddy, N., G. Bossi, K. J. Adams, A. Lissina, T. M. Mahon, N. J. Hassan, J. Gavarret, F. C. Bianchi, N. J. Pumphrey, K. Ladell, et al. 2012. Monoclonal TCR-redirected tumor cell killing. *Nat. Med.* 18: 980–987.
15. Sadelain, M., R. Brentjens, and I. Rivière. 2009. The promise and potential pitfalls of chimeric antigen receptors. *Curr. Opin. Immunol.* 21: 215–223.
16. Thomas, D. A., S. O'Brien, S. Faderl, G. Garcia-Manero, A. Ferrajoli, W. Wierda, F. Ravandi, S. Verstovsek, J. L. Jorgensen, C. Bueso-Ramos, et al. 2010. Chemoimmunotherapy with a modified hyper-CVAD and rituximab regimen improves outcome in de novo Philadelphia chromosome-negative precursor B-lineage acute lymphoblastic leukemia. *J. Clin. Oncol.* 28: 3880–3889.
17. Jaglowski, S. M., L. Alinari, R. Lapalombella, N. Muthusamy, and J. C. Byrd. 2010. The clinical application of monoclonal antibodies in chronic lymphocytic leukemia. *Blood* 116: 3705–3714.
18. Abramson, J. S., and M. A. Shipp. 2005. Advances in the biology and therapy of diffuse large B-cell lymphoma: moving toward a molecularly targeted approach. *Blood* 106: 1164–1174.
19. Jazirehi, A. R., and B. Bonavida. 2005. Cellular and molecular signal transduction pathways modulated by rituximab (rituxan, anti-CD20 mAb) in non-Hodgkin's lymphoma: implications in chemosensitization and therapeutic intervention. *Oncogene* 24: 2121–2143.
20. Hiraga, J., A. Tomita, T. Sugimoto, K. Shimada, M. Ito, S. Nakamura, H. Kiyoi, T. Kinoshita, and T. Naoe. 2009. Down-regulation of CD20 expression in B-cell lymphoma cells after treatment with rituximab-containing combination chemotherapies: its prevalence and clinical significance. *Blood* 113: 4885–4893.
21. Jilani, I., S. O'Brien, T. Manshuri, D. A. Thomas, V. A. Thomazy, M. Imam, S. Naeem, S. Verstovsek, H. Kantarjian, F. Giles, et al. 2003. Transient down-modulation of CD20 by rituximab in patients with chronic lymphocytic leukemia. *Blood* 102: 3514–3520.
22. Tsai, P. C., F. J. Hernandez-Ilizaliturri, N. Bangia, S. H. Olejniczak, and M. S. Czuczman. 2012. Regulation of CD20 in rituximab-resistant cell lines and B-cell non-Hodgkin lymphoma. *Clin. Cancer Res.* 18: 1039–1050.
23. Johnson, N. A., S. Leach, B. Woolcock, R. J. deLeeuw, A. Bashashati, L. H. Sehn, J. M. Connors, M. Chhanabhai, A. Brooks-Wilson, and R. D. Gascoyne. 2009. CD20 mutations involving the rituximab epitope are rare in diffuse large B-cell lymphomas and are not a significant cause of R-CHOP failure. *Haematologica* 94: 423–427.
24. Shimada, K., A. Tomita, S. Saito, and H. Kiyoi. 2014. Efficacy of ofatumumab against rituximab-resistant B-CLL/SLL cells with low CD20 protein expression. *Br. J. Haematol.* 166: 455–457.
25. Uchiyama, S., Y. Suzuki, K. Otake, M. Yokoyama, M. Ohta, S. Aikawa, M. Komatsu, T. Sawada, Y. Kagami, Y. Morishima, and K. Fukui. 2010. Development of novel humanized anti-CD20 antibodies based on affinity constant and epitope. *Cancer Sci.* 101: 201–209.
26. Tomita, A., J. Hiraga, H. Kiyoi, M. Ninomiya, T. Sugimoto, M. Ito, T. Kinoshita, and T. Naoe. 2007. Epigenetic regulation of CD20 protein expression in a novel B-cell lymphoma cell line, RRBL1, established from a patient treated repeatedly with rituximab-containing chemotherapy. *Int. J. Hematol.* 86: 49–57.
27. Sonoki, T., Y. Li, S. Miyanishi, H. Nakamine, N. Hanaoka, H. Matsuoka, I. Mori, and H. Nakakuma. 2009. Establishment of a novel CD20 negative mature B-cell line, WILL2, from a CD20 positive diffuse large B-cell lymphoma patient treated with rituximab. *Int. J. Hematol.* 89: 400–402.
28. van Meerten, T., R. S. van Rijn, S. Hol, A. Hagenbeek, and S. B. Ebeling. 2006. Complement-induced cell death by rituximab depends on CD20 expression level and acts complementary to antibody-dependent cellular cytotoxicity. *Clin. Cancer Res.* 12: 4027–4035.
29. Terakura, S., T. N. Yamamoto, R. A. Gardner, C. J. Turtle, M. C. Jensen, and S. R. Riddell. 2012. Generation of CD19-chimeric antigen receptor modified $CD8^+$ T cells derived from virus-specific central memory T cells. *Blood* 119: 72–82.
30. Lenkei, R., J. W. Gratama, G. Rothe, G. Schmitz, J. L. D'hautcourt, A. Arekrans, F. Mandy, and G. Marti. 1998. Performance of calibration standards for antigen quantitation with flow cytometry. *Cytometry* 33: 188–196.
31. Kumar, A., E. T. Petri, B. Halmos, and T. J. Boggon. 2008. Structure and clinical relevance of the epidermal growth factor receptor in human cancer. *J. Clin. Oncol.* 26: 1742–1751.
32. Wang, X., W. C. Chang, C. W. Wong, D. Colcher, M. Sherman, J. R. Ostberg, S. J. Forman, S. R. Riddell, and M. C. Jensen. 2011. A transgene-encoded cell surface polypeptide for selection, in vivo tracking, and ablation of engineered cells. *Blood* 118: 1255–1263.
33. Szymczak-Workman, A. L., K. M. Vignali, and D. A. Vignali. 2012. Design and construction of 2A peptide-linked multicistronic vectors. Cold Spring Harb. Protoc. 2012(2): 199–204.

34. Andris-Widhopf, J., P. Steinberger, R. Fuller, C. Rader, and C. F. Barbas, 3rd. 2011. Generation of human scFv antibody libraries: PCR amplification and assembly of light- and heavy-chain coding sequences. *Cold Spring Harb. Protoc.* 2011(9).
35. Weijtens, M. E., R. A. Willemsen, B. A. van Krimpen, and R. L. Bolhuis. 1998. Chimeric scFv/gamma receptor-mediated T-cell lysis of tumor cells is coregulated by adhesion and accessory molecules. *Int. J. Cancer* 77: 181–187.
36. Faroudi, M., C. Utzny, M. Salio, V. Cerundolo, M. Guiraud, S. Müller, and S. Valitutti. 2003. Lytic versus stimulatory synapse in cytotoxic T lymphocyte/target cell interaction: manifestation of a dual activation threshold. *Proc. Natl. Acad. Sci. USA* 100: 14145–14150.
37. Oki, Y., J. R. Westin, F. Vega, H. Chuang, N. Fowler, S. Neelapu, F. B. Hagemeister, P. McLaughlin, L. W. Kwak, J. E. Romaguera, et al. 2013. Prospective phase II study of rituximab with alternating cycles of hyper-CVAD and high-dose methotrexate with cytarabine for young patients with high-risk diffuse large B-cell lymphoma. *Br. J. Haematol.* 163: 611–620.
38. Hallek, M., B. D. Cheson, D. Catovsky, F. Caligaris-Cappio, G. Dighiero, H. Döhner, P. Hillmen, M. J. Keating, E. Montserrat, K. R. Rai, and T. J. Kipps, International Workshop on Chronic Lymphocytic Leukemia. 2008. Guidelines for the diagnosis and treatment of chronic lymphocytic leukemia: a report from the International Workshop on Chronic Lymphocytic Leukemia updating the National Cancer Institute-Working Group 1996 guidelines. *Blood* 111: 5446–5456.
39. Prevodnik, V. K., J. Lavrenčak, M. Horvat, and B. J. Novakovič. 2011. The predictive significance of CD20 expression in B-cell lymphomas. *Diagn. Pathol.* 6: 33.
40. Wierda, W. G., S. Padmanabhan, G. W. Chan, I. V. Gupta, S. Lisby, and A. Osterborg, Hx-CD20-406 Study Investigators. 2011. Ofatumumab is active in patients with fludarabine-refractory CLL irrespective of prior rituximab: results from the phase 2 international study. *Blood* 118: 5126–5129.
41. Scott, A. M., J. D. Wolchok, and L. J. Old. 2012. Antibody therapy of cancer. *Nat. Rev. Cancer* 12: 278–287.
42. Turatti, F., M. Figini, E. Balladore, P. Alberti, P. Casalini, J. D. Marks, S. Canevari, and D. Mezzanzanica. 2007. Redirected activity of human antitumor chimeric immune receptors is governed by antigen and receptor expression levels and affinity of interaction. *J. Immunother.* 30: 684–693.
43. Hudecek, M., M. T. Lupo-Stanghellini, P. L. Kosasih, D. Sommermeyer, M. C. Jensen, C. Rader, and S. R. Riddell. 2013. Receptor affinity and extracellular domain modifications affect tumor recognition by ROR1-specific chimeric antigen receptor T cells. *Clin. Cancer Res.* 19: 3153–3164.
44. Haso, W., D. W. Lee, N. N. Shah, M. Stetler-Stevenson, C. M. Yuan, I. H. Pastan, D. S. Dimitrov, R. A. Morgan, D. J. FitzGerald, D. M. Barrett, et al. 2013. Anti-CD22-chimeric antigen receptors targeting B-cell precursor acute lymphoblastic leukemia. *Blood* 121: 1165–1174.
45. Long, A. H., W. M. Haso, and R. J. Orentas. 2013. Lessons learned from a highly-active CD22-specific chimeric antigen receptor. *OncoImmunology* 2: e23621.
46. Casucci, M., B. Nicolis di Robilant, L. Falcone, B. Camisa, M. Norelli, P. Genovese, B. Gentner, F. Gullotta, M. Ponzoni, M. Bernardi, et al. 2013. CD44v6-targeted T cells mediate potent antitumor effects against acute myeloid leukemia and multiple myeloma. *Blood* 122: 3461–3472.
47. Tang, Y., J. Lou, R. K. Alpaugh, M. K. Robinson, J. D. Marks, and L. M. Weiner. 2007. Regulation of antibody-dependent cellular cytotoxicity by IgG intrinsic and apparent affinity for target antigen. *J. Immunol.* 179: 2815–2823.

OncoImmunology 4:2, e988098; February 2015; © 2015 Taylor & Francis Group, LLC

Oncolytic virus expressing RANTES and IL-15 enhances function of CAR-modified T cells in solid tumors

Nobuhiro Nishio[1] and Gianpietro Dotti[1,2,3,*]

[1]Center for Cell and Gene Therapy; Baylor College of Medicine; Houston, TX USA; [2]Department of Immunology; Baylor College of Medicine; Houston, TX USA; [3]Department of Medicine; Baylor College of Medicine; Houston, TX USA

Keywords: chimeric antigen receptor, GD2 antigen, IL-15, oncolytic virus, RANTES

We improved the migration and survival of chimeric antigen receptor (CAR)-modified T cells in solid tumors by combining CAR-T cells with an armed oncolytic virus. Local delivery of the chemokine RANTES and the cytokine IL-15 by the oncolytic virus enhanced the trafficking and persistence of the CAR-T cells, resulting in improved antitumor effects.

Adoptive transfer of T cells modified to express chimeric antigen receptors (CARs) has had clinical success in B-lymphocyte derived malignancies.[1] However, the clinical efficacy of CAR-T cells remains limited in solid tumors. This unfavorable outcome could be due to the insufficient migration of the infused T cells to the tumor site as well as to the immunosuppressive characteristics of the tumor environment that inhibits the effector function and proliferation of those few T cells that do reach the tumor.

CAR molecules have been further engineered to express co-stimulatory endodomains such as those derived from CD28 and tumor necrosis factor receptor superfamily member 9 (TNFRSF9, better known as 4–1BB) to promote T-cell proliferation and persistence upon encountering tumor cells. CD28 has proven effective in inducing CAR-T cell expansion in B-cell malignancies.[2,3] The incorporation of 4–1BB seems, however, to sustain more robust engraftment of CD19-specific CAR-T cells.[1] The incorporation of these co-stimulatory molecules in CARs targeting antigens expressed by solid tumors is anticipated to play a similarly crucial role.

CAR-T cells targeting CD19 seem to traffic physiologically to the bone marrow and lymph nodes, the primary sites of hematologic malignancies.[1,3] In addition, they can encounter both normal B lymphocytes and leukemic cells directly in the circulation. By contrast, T-cell migration remains a relevant problem for solid tumors. For instance, while tumor-infiltrating T lymphocytes (TILs) isolated from tumor biopsies and expanded *ex vivo* show dramatic migration to melanoma lesions, polyclonal T lymphocytes isolated from the peripheral blood and engineered with a T-cell receptor seem less effective. This disparity suggests that TILs and peripheral blood T cells may have a different pattern of homing molecules.[4] If the current CAR-T cell studies in solid tumors such as neuroblastoma, prostate cancer, pancreatic cancer, and mesothelioma reveal suboptimal migration, countermeasures to increase T-cell migration should be applied. Radiation or chemotherapy before the infusion of CAR-T cells in patients with solid tumors may favorably alter the pattern of T-cell migration. However, several preclinical models have already demonstrated that engineering CAR-T cells to express chemokine receptors that pair with chemokines produced by tumor cells is a strategy that can overcome the trafficking issue.[5]

When CAR-T cells reach the tumor bed in a sufficient number, tumor-associated inhibitory mechanisms are there to shutdown effective immune responses. In the treatment of small tumors, infusion of CAR-T cells after chemo or radiotherapy may partially reduce the impact of these inhibitory mechanisms. In addition, the recent introduction of antibodies that block T-cell inhibitory mechanisms, such as those abrogating the immune checkpoint CTLA-4 and PD1-PDL-1 pathways, shows great potential. Combinations of CAR-T cell therapies with these antibodies are anticipated to make a substantial difference in the near future. Similarly to the genetic modification of CAR-T cells aimed to express specific chemokine receptors, a plethora of genetic modifications has been proposed to increase the fitness of CAR-T cells within the tumor environment.[5] Some of the proposed modifications are currently under clinical investigation. Although each single modification seems to have specific beneficial effects, multiple mechanisms of resistance can be developed by tumors. T cells must accomplish simultaneously optimal trafficking and persistence, while also retaining an acceptable safety profile. In our recent study,[6] we developed an engineering strategy where an armed oncolytic virus (OV), another single biological agent, creates a favorable tumor environment for CAR-T cells.

OVs selectively infect, lyse and replicate in malignant cells without affecting non-malignant cells.[7] In addition, OVs

*Correspondence to: Gianpietro Dotti; Email: gdotti@bcm.edu
Submitted: 11/08/2014; Accepted: 11/12/2014
http://dx.doi.org/10.4161/21505594.2014.988098

have sufficient cargo capacity to insert multiple ectopic genes that can be beneficial for CAR-T cells. To investigate the effect of combining armed OV and CAR-T cells, we choose the neuroblastoma model since this tumor model has been previously targeted with CAR-T cells specific for the GD2 antigen.[8] We also selected an oncolytic adenovirus (Ad5Δ24) that has been extensively used in the clinic. We exploited the tropism of the OV for the tumor cells and engineered the virus to express both a chemokine and a growth factor for the T cells in order to achieve optimal trafficking of the engineered T cells to the tumor site and to generate a cytokine milieu that sustains T-cell growth and survival. Therefore, we armed Ad5Δ24 with chemokine (C-C motif) ligand 5 (CCL5, better known as RANTES) and interleukin (IL)-15 (**Fig. 1**), 2 immunomodulatory molecules selected on the basis of both clinical and preclinical data. RANTES is also a very potent chemokine and its receptors are maintained in T cells expanded *ex vivo*. Using this strategy, we anticipated that tumor cells, regardless of their tissue origin, could be forced to ectopically express RANTES after infection with the armed OV. We hypothesized that this strategy would promote efficient migration of the infused CAR-T cells without the need to select a chemokine/chemokine receptor pathway specific for each single tumor type. The cytokine IL-15 was selected for its multiple beneficial effects on T cells, and its overall ability to increase T-cell antitumor functions. In our experimental design, we demonstrated that neuroblastoma cells infected with Ad5Δ24.RANTES.IL-15 produce functional levels of RANTES and IL-15 both *in vitro* and *in vivo*, while the cytopathic effect of the virus is conserved. In a xenogenic mouse model, combined therapy with Ad5Δ24.RANTES.IL-15 and GD2.CAR-T cells significantly enhanced the survival of mice as compared with either of the monotherapies. Furthermore, both RANTES and IL-15 released by the armed OV were predominantly detected at the tumor site, rather than in the serum, indicating a preferential local expression of both factors. This strategy thereby circumvented the toxicities associated with systemic administration of cytokines.[6]

In conclusion, our preclinical study demonstrates that optimal trafficking and survival of CAR-T cells can be obtained in solid tumors by engineering an OV without compromising its cytopathic effect. In principle, similar genetic modifications can be applied to OVs such as vaccinia viruses and measles virus that have been administered intravenously into patients to treat metastatic tumors already.[9,10] Arming these viruses using this proposed strategy will not only favor the rapid recruitment of tumor-specific T cells to the primary lesions so infected but will also enhance the spread of the virus to other tumor cells, thus amplifying the therapeutic effect of the viruses. In addition, considering the cargo capacity of these viruses, other relevant genes that may further overcome inhibitory mechanisms can be accommodated.

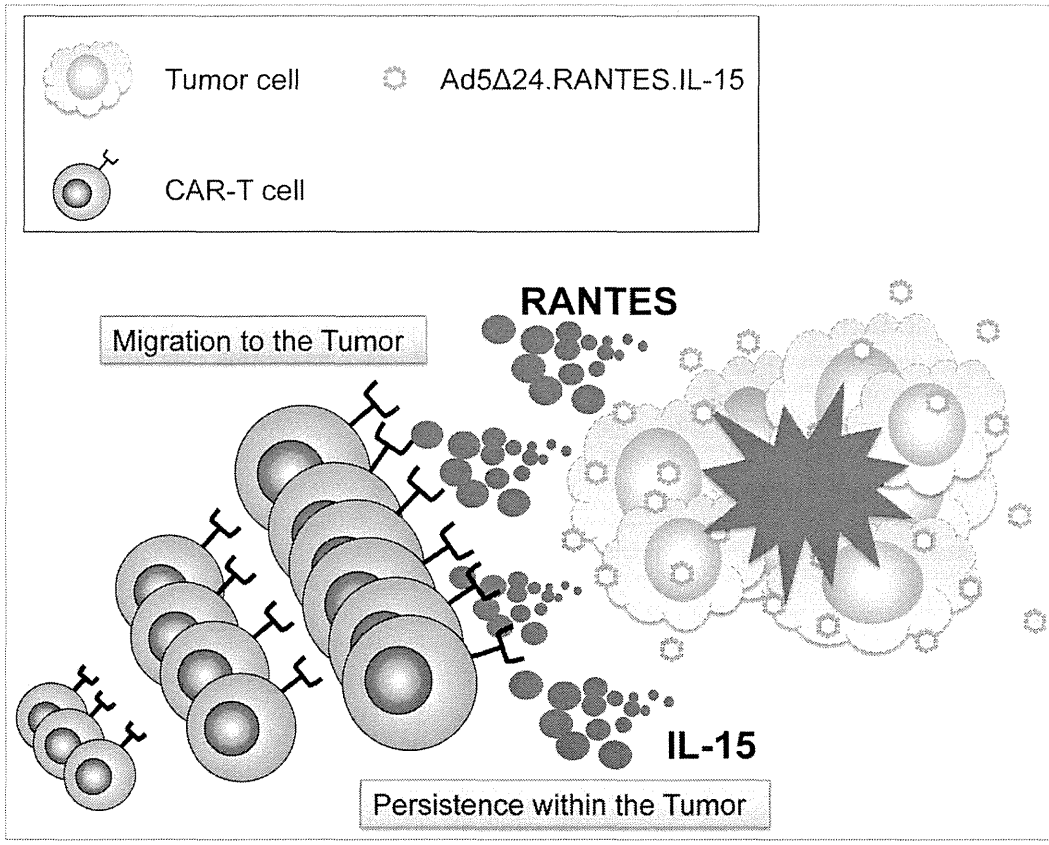

Figure 1. Combined therapy with CAR-T cells and Ad5Δ24 armed with RANTES and IL-15. Oncolytic viruses (OVs) selectively infect and lyse tumor cells, and then spread to neighboring tumor cells. Virus-infected tumor cells release both proteins and undergo apoptosis. The chemokine RANTES attracts circulating chimeric antigen receptor (CAR) modified T cells (CAR-T) to the virus infected tumor site and migrated CAR-T cells persist by virtue of interleukin 15 (IL-15) and specific antigen stimulation.

Disclosure of Potential Conflicts of Interest

No potential conflicts of interest were disclosed.

Acknowledgment

The authors would like to thank Catherine Gillespie for editing the invited auto commentary.

Funding

This work was supported in part by R01 CA142636 National Institute of Health-NCI and W81XWH-10–10425 Department of Defense and Technology/ Therapeutic Development Award.